Characterization of Electrically Controlled Gel Polymer Electrolyte Monopropellants

Harrison R. Autry

Thesis submitted to the faculty of the
Virginia Polytechnic Institute and State University
in partial fulfillment of the requirements for the degree of

Master of Science
In
Aerospace Engineering

Gregory Young, Chair
Gary D. Seidel
Luca Massa

April 19, 2023
Blacksburg, Virginia

Keywords: Rocket Propulsion, Monopropellant, Gel, Gel Polymer Electrolyte, Electrolysis

Characterization of Electrically Controlled Gel Polymer Electrolyte Monopropellants

Harrison R. Autry

ABSTRACT

Increasing interest in the development of nontoxic monopropellants for the replacement of hydrazine and its derivatives stems from the desire for safer and thus more cost-effective alternatives. Ionic liquid monopropellants based on the hydroxylammonium nitrate and ammonium dinitramide ionic oxidizer salts have received the majority of attention over the last two decades and present a promising alternative with higher performance and more attractive handling qualities than hydrazine. These monopropellants are employed using catalytic methods which lead to their decomposition and ignition. However, the development of compatible catalysts remains a limiting step in the technological readiness of these alternative monopropellants. Due to their ionic nature, the development of ionic liquid monopropellants has led to many investigations on the utilization of electrolysis to achieve combustion.

Separately, there has been a longtime interest in the use of gelled propellants for enhanced handling and operating safety. Atomization and combustion inefficiencies associated with gels have continued to limit their use. Monopropellants composed of gel polymer electrolytes present a unique opportunity which combines the safety features of gelled propellants as well as the ionic conductivity seen in ionic liquids, allowing them to decompose and ignite electrolytically. In this research, a family of electrically controlled monopropellants that utilize electrolysis in this fashion was developed from a gel polymer electrolyte. Their fundamental properties, including those pertaining to rheology, conductivity, thermal stability, and combustion, are explored as the composition of the oxidizer salt is varied.

Characterization of Electrically Controlled Gel Polymer Electrolyte Monopropellants

Harrison R. Autry

GENERAL AUDIENCE ABSTRACT

Current advancements in rocket propulsion include interests in developing alternative green propellants for use in spacecraft propulsion systems with the hope of replacing current options which may be toxic to handle and present a serious safety hazard. Alternative propellants are generally thought of as not requiring special safety equipment or protocols in their handling, thereby reducing costs. Several promising options belonging to a category of propellants known as ionic liquids have made significant progress in development since the 1990s and have the potential to be used alongside a novel electrical combustion method known as electrolysis. Gelled propellants are another possible alternative which have been researched for their appealing safety qualities for some time.

While not researched for their use as rocket propellants until very recently, gel polymer electrolytes have received interest in this application due to their composition which includes a polymer, commonly used as rocket fuel, and an oxidizer salt. Due to their inherent electrical conductivity, their potential to use electrolysis in a similar manner to ionic liquids to achieve combustion is of interest. The research detailed in this thesis was completed to characterize fundamental material and combustion properties of a gel polymer electrolyte propellant as its oxidizer constituents are varied.

Dedication

This work is dedicated to all of the family, friends, and colleagues that have encouraged and supported me through the last six years. I am tremendously grateful to have you in my life.

Acknowledgements

I would like to acknowledge and thank my advisor, Dr. Greg Young, for providing me with this opportunity to pursue and explore rocket propulsion in an experimental setting. While difficult at times, this experience has been extremely exciting and fulfilling. My appreciation for his guidance and tutelage cannot be overstated.

I'd like to thank my advisory committee, Dr. Gary Seidel and Dr. Luca Massa, for their support and feedback.

In addition, I'd like to thank several research colleagues that have helped guide me over the last three semesters: Brad Gobin, Sean Whalen, and Dominic Gallegos. I greatly appreciate the useful insight and discourse that have contributed to my experience in this group.

The research detailed in this thesis was conducted with the support of the Air Force Office of Scientific Research under grant FA9550-21-1-0265. This work was made possible by the use of Virginia Tech's Materials Characterization Facility, which is supported by the Institute for Critical Technology and Applied Science, the Macromolecules Innovation Institute, and the Office of the Vice President for Research and Innovation.

Thank you all.

Table of Contents

List of Figures

List of Tables

List of Symbols and Abbreviations

AC	Alternating Current
ACN	Acetonitrile
ADN	Ammonium Dinitramide
A_e	Nozzle Exit Plane Area
AFRL	Air Force Research Laboratory
AMCOM	U.S. Army Aviation and Missile Command
AP	Ammonium Perchlorate
CEA	Chemical Equilibrium with Applications
DC	Direct Current
DLR	German Aerospace Center
DSC	Differential Scanning Calorimetry
ECP	Electrically Controlled Propellant
ECGP	Electrically Controlled Gel Propellant
ECSP	Electrically Controlled Solid Propellant
EIS	Electrochemical Impedance Spectroscopy
FMTI	Future Missile Technology Integration
FOI	The Swedish Defense Research Agency
FRA	Frequency Response Analyzer
GALCIT	California Institute of Technology Guggenheim Aeronautical Laboratory

GPE	Gel Polymer Electrolyte
GRM	Gel Rocket Motor
HAN	Hydroxylammonium Nitrate
HMIS	Hazardous Materials Identification System
HTPB	Hydroxyl-Terminated Polybutadiene
IRFNA	Inhibited Red Fuming Nitric Acid
IL	Ionic Liquid
I_{sp}	Specific Impulse
I_{vac}	Vacuum Specific Impulse
JATO	Jet-Assisted-Take-Off
LiCl	Lithium Chloride
LP	Lithium Perchlorate
$\dot{m}$	Propellant Mass Flow Rate
MDI	Methylene Diphenyl Diisocyanate
NASA	Naional Aeronautics and Space Administration
NFPA	National Fire Prevention Association
p_a	Pressure in Ambient Atmosphere
p_e	Pressure at the Nozzle Exit Plane
PDL	Pressure Deflagration Limit
PE	Polymer Electrolyte
PEG	Polyethylene Glycol
PEO	Polyethylene Oxide
SMD	Sauter Mean Diameter

SPE	Solid Polymer Electrolyte
SRM	Solid Rocket Motor
$\mathcal{T}$	Thrust Force
TGA	Thermogravimetric Analysis
u_e	Nozzle Exit Plane Velocity
u_{eq}	Equivalent Exhaust Velocity

1. Introduction

Rocket propulsion systems are used in missions designed to operate in an environment deficient of air, such as space, as well as over long ranges in trans-atmospheric flight conditions. Typical applications include space launch vehicles, spacecraft propulsion systems, satellite station keeping, and in defense applications as missiles. A type of liquid propellant, known as a monopropellant, is commonly used for auxiliary spacecraft propulsion systems for maneuvering, attitude control, and station keeping.

The research detailed in this thesis focuses on the exploration of material and combustion characteristics of a family of gel monopropellants that are made of a gel polymer electrolyte and use electrochemical means to decompose and ignite. This chapter briefly covers the categorization of rocket propulsion systems as well as their respective historical development and uses as a means to provide a background and motivation for the research laid forth in this thesis. Chapter 2 will review literature pertaining to research conducted on relevant topics and chapter 3 will provide insight to the procedure and methods used in preparing and conducting the experimental characterization of the material and combustion characteristics of the family of gel polymer electrolyte monopropellants. Chapters 4 and 5 analyze the results of these experiments.

1.1. Classification of Propulsion Systems

The concept of jet propulsion generally refers to the motion of a body resulting from a reactionary force to the momentum of ejected matter and can be classified as rocket propulsion or duct propulsion [1]. Rocket propulsion systems are those which expel a stored propellant to produce momentum, while duct propulsion, which includes air-breathing engines, achieves this in the combustion of onboard fuel with atmospheric air [1]. Duct propulsion systems are

categorized into those with turbomachinery, including turbojets and turbofans, and those without turbomachinery, including ramjets and scramjets [1][2].

1.2. Rocket Propulsion Systems

When compared to airbreathing propulsion systems, the high thrust-to-weight ratio and use of a stored oxidizer in the propellant of a rocket presents an opportunity for very long flight ranges as well as operation in environments that are lacking in air, such as the upper atmosphere and space [1].

Rocket propulsion systems can be categorized based upon their source of energy [1][2]. Chemical rocket propulsion is one such category that uses the expansion of the high temperature gaseous products of propellant combustion through a nozzle to achieve thrust [1]. This category can further be divided based on the propellant type. Propellants, consisting of fuel and oxidizing chemicals, can be solid, liquid, or a combination of the two, which is seen in hybrid-propellant rockets [1].

An important parameter to consider that indicates the performance of a rocket system is its specific impulse (I_{sp}), which is a parameter derived from the rocket thrust equation, found in Equation 1.1 [1][2].

$$\mathcal{T} = \dot{m}u_e + (p_e - p_a)A_e \qquad \textbf{(1.1)}$$

Here, $\mathcal{T}$ is the thrust, $\dot{m}$, is the mass flow rate of propellant from the rocket, u_e is the velocity of fluid exiting the rocket nozzle, p_e is the pressure at the exit plane of the rocket nozzle, p_a is the atmospheric pressure, and A_e is the area of the exit plane of the nozzle. A term called the

equivalent exhaust velocity is defined u_{eq} in Equation 1.2 and allows us to write the I_{sp} as it appears in Equation 1.3, where g_e is the acceleration due to gravity at the surface of the Earth [2].

$$u_{eq} = \frac{\mathcal{T}}{\dot{m}} = u_e + \frac{(p_e - p_a)}{\dot{m}} A_e \quad \textbf{(1.2)}$$

$$I_{sp} = \frac{u_{eq}}{g_e} \quad \textbf{(1.3)}$$

The specific impulse is the total impulse of the vehicle per unit mass of propellant, which is a measurement that is indicative in a sense of a rocket's propellant efficiency [2].

1.2.1. Historic Development of Rocket Propulsion

Rockets that utilize a solid propellant are considered the oldest form of jet propulsion with the use of gunpowder to propel fireworks dating back as early as the twelfth century in China. Over the ensuing centuries, various civilizations worked to develop solid rockets for use in combat. By the eighteenth and nineteenth centuries, the use of solid propellants in missiles was common [2]. More modern development in solid propellants originated with Dr. Theodore von Karman's group at the California Institute of Technology Guggenheim Aeronautical Laboratory (GALCIT) beginning in the 1930s [3]. By 1942, this group received funding to develop jet-assisted-take-off (JATO) motors, and in March of that year, they moved off campus to become the Aerojet Engineering Corporation [3]. This group also developed the concept of casting solid propellants directly into their motor case, as opposed to propellants that are inserted as a cartridge into the case [3]. They initially used an asphalt fuel binder with potassium perchlorate oxidizer but would

later move on to polyester, and then polyurethane fuels as a replacement for asphalt. Other companies, namely Thiokol, also worked to develop rubber fuel binders. Recent developments have focused on the enhancement of the motor cases and nozzles with composite materials to withstand increasing burn times and flame temperatures, as well as support the capabilities of variable thrust, vectoring, termination, and restart [3]. Liquid propellants do not have as long a history, with their inspiring development taking place solely over the previous century. They were pioneered by a few individuals spanning the globe through the first half of the 20th century. The use of liquid propellants was first proposed in 1903 by Konstantin Tsiolkovsky, an unknown schoolteacher from the Kaluga Province of Russia, who published such an idea in an article titled "Exploration of Space with Reactive Devices". He recognized that a solid gunpowder rocket would not be energetic enough to exit the atmosphere, and instead suggested the possibility of space travel with the use of liquid oxygen as an oxidizer and liquid hydrogen as a fuel. Tsiolkovsky did not complete any experimentation, and his work drew little attention, remaining unknown outside of Russia until it was republished in Germany about two decades later [2,4]. Robert Goddard, an American physics professor, separately recognized advantages with liquid oxygen and liquid hydrogen in propulsion. He went on to conduct experiments between the 1920s and 1930s with liquid oxygen and gasoline propellants, flying the first liquid propellant rocket in 1926 [4]. During his life, he amassed numerous patents for combustion chambers, propellant feed systems, and multistage rockets. Herman Oberth of Germany conducted similar assessments of liquid propellants utilizing fuels of liquid hydrogen and alcohol [2]. His book, "The Rocket into Planetary Space", published in 1923, inspired many around the world to take an interest in rockets and space travel, and gave rise to space societies over the next decade that assumed the responsibility of lecturing and writing books on these topics. Additional people that

contributed to the early development of liquid propellants include Luigi Crocco of Italy and V.P. Glushko of Russia, who separately became the first people to utilize an oxidizer other than liquid oxygen in 1930 by employing nitrogen tetroxide, which is stable in storage at room temperature. Methane, kerosene, and a blend of ethyl alcohol and water were introduced as fuels in propellant applications over the following years. The latter was successfully fired with liquid oxygen as oxidizer in early 1932; this formulation would serve as the basis of the propellant that powered the first long-range ballistic missile in World War II, which was the German A-4, more commonly known as the V-2 [4].

The previously mentioned Crocco also became an early contributor to the development of monopropellants, which present the opportunity for simpler and cheaper systems in comparison to those required by the bipropellants developed thus far. He first experimented with nitroglycerine and methyl alcohol mixtures before moving on to the less sensitive nitromethane, producing promising results before his funding concluded in 1935. Another contributor was Helmuth Walter of the Chemical State Institute in Berlin. Though his work was kept private by the Luftwaffe of Nazi Germany, Walter developed a monopropellant that used the newly available 80% concentration hydrogen peroxide, which he found decomposed into oxygen and superheated steam upon catalyzation or proper heating. This monopropellant was employed by Werner Von Braun in driving the fuel pumps of the A-4 missile, where he used a calcium permanganate solution as a catalyst [4].

Globally, the development of liquid and solid rockets throughout World War II and during the two decades following was primarily motivated by military and defense needs. This motivation changed in 1957 with the emergence of the space race, as the Soviet Union successfully launched the first artificial satellite into orbit on October 4 of that year. In 1961, the United States began

their program aimed at setting foot on the moon. Over the next eight years, they developed the necessary means to do so, and completed this mission in 1969 with Apollo 11. [2] Continuing development since this era has brought solid and liquid propulsion systems to high levels of performance and is incentivized by the sustained presence of satellites and spacecraft in space for communication, defense, and exploratory purposes.

1.2.2. Solid Rocket Motors

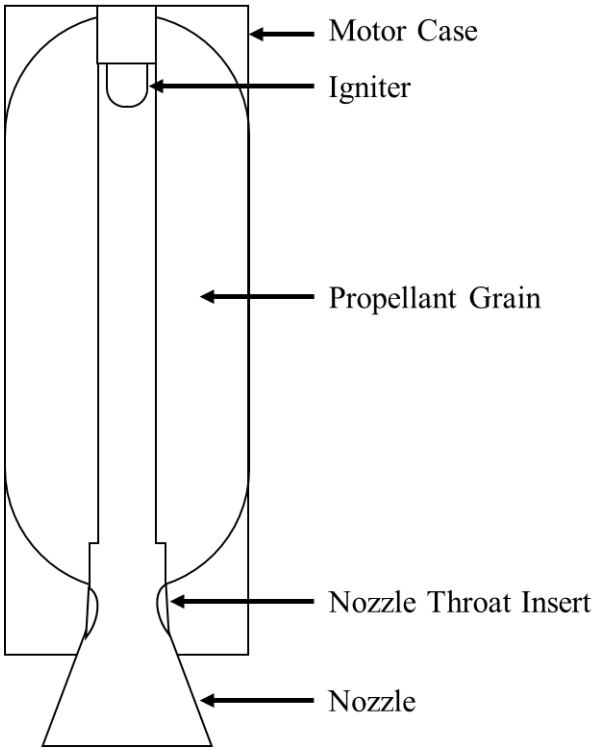

Figure 1.1: A simplified SRM schematic adapted from [1].

A solid propellant grain is composed of a homogenous compound, where the fuel and oxidizer components exist in the same molecule, or a composite mixture that contains oxidizer particles held together by a polymer binder that acts as fuel. Metal powders such as aluminum are typically added in composite propellants to increase performance [1,2]. The propellant burns at

rates depending on the combustion chamber temperature and pressure and can produce a variable thrust profile depending on the grain geometry [2]. A solid rocket motor (SRM) stores this propellant directly in the combustion chamber of the vessel, simplifying both the design of the motor and its integration with payload and vehicles. A simplified schematic of a SRM can be found in Figure 1.1. Due to the higher density of solid propellants in comparison to that of liquid propellants, the use of a SRM can allow for a smaller overall vehicle that experiences less drag [1]. The propellant is stable in long term storage from 10 to 30 years with no possibility of leakage [1]. While SRMs can have extinctions and multiple burns included in its design, these are limited and do not allow for random throttling with an external input [1]. Because of the solid propellant's composition of both oxidizer and fuel in a continuous mass, the likelihood of explosion and catastrophic failure can be high, and they can be detonable in the cases of simple impact if mishandled and dropped or if the motor is penetrated by a bullet [1-3]. Common applications of SRMs today include boosters and second stage motors of space launch vehicles, tactical missiles and missile defense, and gas generators for various purposes, such as short-term power supply and air bag deployment [1,2].

1.2.3. Liquid Rocket Engines

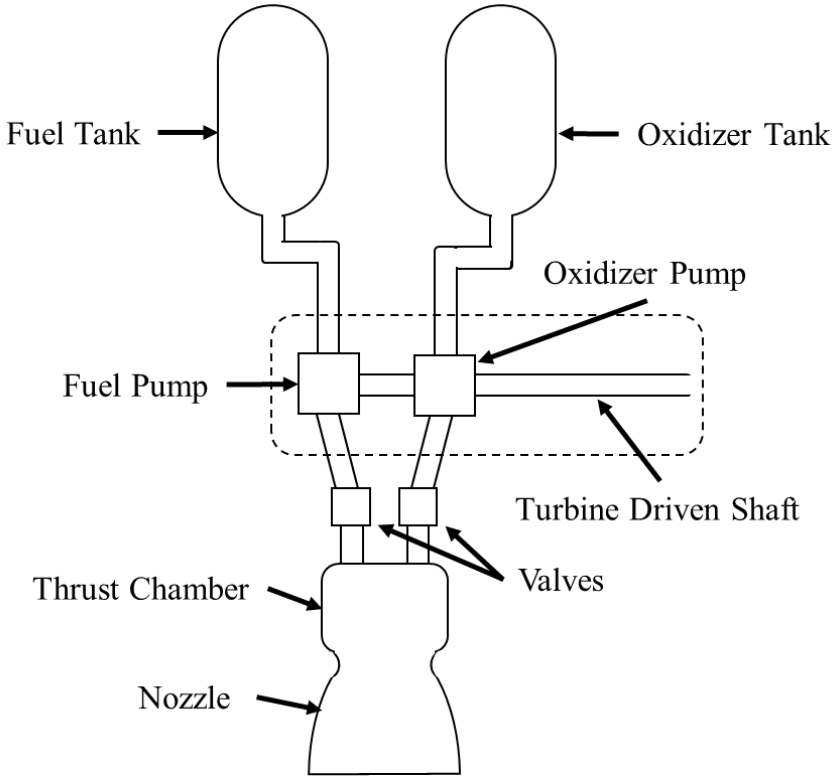

Figure 1.2: A simplified type of liquid rocket engine adapted from [1].

Liquid propellants are categorized into monopropellant and bipropellant systems [1]. These systems can be further classified by their propellants, application, staging, or their propellant feed mechanism [1]. The combustion device used in a liquid rocket engine is known as the thrust chamber, which is composed of injectors, a combustion chamber, and a nozzle [1]. The propellant is fed via pressurization or turbopumps from their separate storage tanks, through the injectors, and into the combustion chamber to be ignited [1][2]. The gaseous combustion products are expanded through the nozzle to provide thrust [1]. A depiction of a representative liquid rocket engine that utilizes turbomachinery as a propellant feed mechanism can be found in Figure 1.2. Common liquid propellants include oxidizers such as liquid oxygen, nitric acid, or nitrogen tetroxide, and fuels such as liquid hydrogen, kerosene, and alcohol [1][4]. It is common

to use fuel as a source of cooling for the thrust chamber, where it is circulated through passages in the nozzle [1][2][4].

Bipropellant systems have separately stored fuel and oxidizer which are combined and ignited in the combustion chamber [1][2][4]. These propellants can be hypergolic, where ignition occurs upon contact of the oxidizer and fuel, or nonhypergolic, which requires an ignition system [1][2]. The combustion of certain liquid propellants results in the highest specific impulse of rocket propulsion systems, leading to increased vehicle velocities, and many propellants used also produce nontoxic exhaust which presents low risk to the environment [1]. Liquid rocket engines can also be readily throttled and extinguished and have the ability to be vectored to provide directional control if desired [1,2]. Additionally, liquid systems are often readily reusable [1]. The numerous parts required for feed mechanisms and cooling systems, however, leads to a very complex design, and propellants can easily spill, which becomes increasingly hazardous with particularly volatile options [1,2]. Cryogenic propellants, like liquid oxygen and liquid hydrogen, are not easily storable either, as they are likely to escape as vapors [1]. While the separation of oxidizer and fuel in the bipropellant configuration decreases the likelihood of accidental ignition and catastrophic failures, penetration of a bullet will result in propellant leakage [1]. A comprehensive list of advantages and disadvantages of liquid propellants against those for solid propellants can be found in Table 1.1 and Table 1.2, respectively. Applications for liquid rocket engines include booster and upper stages of space launch vehicles, as well as auxiliary propulsion systems such as attitude control systems in spacecrafts, satellites, and antiballistic missiles [1,2,4].

Table 1.1: Advantages of solid and liquid propulsion systems [1][2].

Advantages of a solid propellant
Simple design with few moving parts.
Easy operation.
No possibility of leakage or spilling of propellant.
Long term storability (10-30 years).
Higher density and density specific impulse, which can lead to smaller vehicles that experience less drag.
Can be designed to achieve termination and reignition to a limited extent.
The use of ablative material in the insulation and nozzle contributes to total impulse.
With the use of a pintle, can achieve a degree of throttling by varying the nozzle throat area.
Can have thrust vector control (TVC) for the cost of simplicity.
Can be designed to be recovered, refurbished, and reused.
Advantages of a liquid propellant
Can achieve highest I_{sp} of available rocket systems.
Ability to be randomly throttled, terminated, and restarted with external input.
External control of thrust-time profile allows for reproducible flight trajectories.
Can be tested and verified at full thrust on the ground before flight.
Can be designed for reuse upon post-flight inspection and servicing as opposed to refurbishment.
Most propellants have nontoxic exhaust.
One propellant feed system can supply multiple thrust chambers in the vehicle.
Can have component redundancy to improve reliability.
Can operate in engine-out scenarios in multiple engine configurations.
Improved flight stability with the placement of fuel and oxidizer tanks to minimize the travel of the vehicle's center of gravity.

Table 1.2: Disadvantages of solid and liquid propulsion systems [1][2].

Disadvantages of a solid propellant
Larger potential for explosions, fires, and catastrophic failure.
Propellant grain can be detonable in certain conditions.
May require environmental permits and safety features for transportation in public conveyance.
Refurbishment requires extensive rework of the motor and new propellants.
Thermal and stress cycling in storage can lead to degradation of the propellant grain.
To implement throttling and stop and restart capabilities, additional ignition systems and increased complexity are required.
Exhaust gases are typically toxic.
Structural integrity of the grain can be difficult to determine once cast; cracks and delamination of the grain can lead to catastrophic failures.
Thrust and operation varies with initial temperature of propellant grain, leading to variability in performance.
Cannot be hot fired on the ground prior to flight of motor.
Disadvantages of a liquid propellant
More complex design in comparison to SRM resulting from fuel and oxidizer tanks, feed systems, pressurization systems, cooling systems, and other necessary engine components.
Cryogenic propellants escape as vapors and cannot be stored for long durations.
Spills and leaks of propellant can be potentially hazardous.
Tanks must be pressurized by a separate pressurization subsystem, increasing the weight of vehicle.
Less dense propellants and packaging of engine components requires more volume and increases the weight of the vehicle.
Sloshing of propellants in their respective tanks can lead to flight instability.

Monopropellants are liquid propellants that possess both oxidizer and fuel components in one compound, either as a mixture or in the same molecule, and ignites upon the decomposition of the compound, which typically occurs due to catalytic or thermal means [1,2,5].

Monopropellants are an appealing alternative to bipropellant systems in many applications because they share many advantages, such as the ability to be throttled as well as terminated and restarted on command in a simpler and more cost-effective package, as only one fluid must be transported to the combustion chamber [5].

1.2.4. Current State of Monopropellants

As mentioned previously, monopropellants are extensively used for attitude and trajectory control thrusters in spacecraft. Various compounds have been historically investigated and high-test hydrogen peroxide was used for a time in small thrusters [1]. However, hydrazine has remained the choice monopropellant since its first flight in 1966 in the upper stage of Titan I due to its proven reliability and performance over decades of use [6].

Hydrazine as a monopropellant is catalyzed most commonly with the Shell 405 spontaneous catalyst, which is composed of an aluminum oxide carrier and iridium activation metal. Once the monopropellant passes over this catalyst, it decomposes in an exothermic reaction to produce ammonia, nitrogen, and hydrogen gases [5]. These hot gases produce thrust as they exit the combustion chamber, producing a specific impulse ranging from 220 to 240 seconds [1]. A monopropellant catalyst can be preheated to obtain almost instantaneous ignition; however, hydrazine becomes catalyzed by certain common materials at elevated temperatures, making material selection for thrusters an important consideration [1,5,7]. Several additional disadvantages have prompted interest and funding in the research of alternative monopropellants

since the 1990s, most notably its high toxicity and flammability in the presence of air which drive handling costs, as well as its high freezing point of about 2°C, which can require its tanks and feeding systems to be electrically heated in cold operating conditions [1,5,6,8,9].

1.2.5. The Search for Alternatives to Hydrazine

The toxicity and carcinogenic nature as well as the associated handling costs in the use of hydrazine is a primary motivator in the search of non-toxic and green monopropellant alternatives [8,10]. While there are no strict definitions of "non-toxic" and "green", Marshall and Deans provide the recommendations and goals that these alternatives meet National Fire Prevention Association (NFPA) and Hazardous Materials Identification System (HMIS) levels lower than that of hydrazine, while also attaining similar performance in terms of specific impulse without the need of exotic materials [10]. Additionally, they should qualify for transportation methods to be shipped in bulk quantities by cargo rail or air, with commercial methods being preferrable [10]. Green monopropellant alternatives include nitrous oxide, hydrogen peroxide, and those based on the ammonium dinitramide (ADN) and hydroxylammonium nitrate (HAN) oxidizer salts [6,11].

ADN and HAN based monopropellants are ionic liquid (IL) blends including water and compatible fuel additives [8-12]. ADN was originally synthesized in Moscow in 1971 and kept classified until rediscovered in the United States in 1988 [8]. The Swedish Defense Research Agency, FOI, began work to develop high performance propellants based on ADN in the early 1990s, resulting in the formulations of LMP-103S and FLP-106 [7,8]. HAN was originally examined by the U.S. Army in research for use as a constituent in the liquid gun propellant (LGP), XM-46, which dates back to the 1970s [13]. Several groups experimented with XM-46 as

a rocket propellant as well, however, this specific formulation was found to be outperformed by other HAN based propellants [13,14]. In 1998, the HAN based AF-M315E was invented at the United States Air Force Research Laboratory (AFRL) [11].

Ionic liquids have reached great strides in development since the 1990s, with AF-M315E, LMP-103S, and FLP-106 exceeding the performance of hydrazine thrusters in both specific impulse, density impulse, and temperature[11,12]. This comparison can be found in Table 1.3. Additionally, these blends do not have toxic vapor pressures, present a lower flammability hazard, and have lower freezing points than hydrazine. Primary drawbacks include their strong oxidizer quality which can affect material considerations, the evaporation of certain constituents when exposed to air, such as ammonia in ADN blends, and their requirement of dedicated manufacturing which leads to increased production costs [11]. The use of HAN and ADN based solutions have been demonstrated with catalytic ignition methods, and due to their ionic nature, electrolytic decomposition and ignition methods have been investigated in research settings as well.

Table 1.3: A comparison of AF-M315E, LMP-103S, FLP-106, and Hydrazine monopropellants [6-8,11,13]

Properties	AF-M315E	LMP-103S	FLP-106	Hydrazine
Density, kg/m^3	1470	1250	1357	1000
Min. Temp (K)	263	266	273	275
I_{sp} (s)	257	252	259	240
Flame Temp (K)	2200	1650	1900	630

1.2.6. Electrolysis

Electrolysis encompasses the electrochemical reactions that ionic materials undergo in the application of a voltage potential. This concept has been proposed as a method to achieve ignition in hydrazine propellants as early as 1975, and current research efforts exist to demonstrate its viability as an alternative to the use of catalysis to achieve ignition in ionic liquids [15]. Potential benefits in using this method to ignite propellants include lower ignition temperatures, reduced power requirements, increased reliability and reusability, and lower overall costs [15].

1.2.7. Interest in Gel Propulsion Systems

According to the International Union of Pure and Applied Chemistry (IUPAC), a gel can be defined from a chemical standpoint as a solid colloidal or polymeric network containing a liquid throughout its volume [16]. They are thixotropic, or shear-thinning semisolid materials with a yield stress which result from the addition of gellants to liquids and they tend to flow similar to a liquid upon the application of a pressure gradient or shear force [17,18]. Their use in propulsion systems has great appeal in their advantages which they inherit from both liquid and solid rocket propellant options. From solid rocket propellants, these include long term storability, reduced possibility of leakage and hazardous vaporization, and great energy density with the ability to suspend metal additives due to the presence of yield stress; from liquids, gel propellants derive an ability to be throttled, extinguished and restarted upon command, insensitivity to impact, and have comparable overall performance [17]. Drawbacks include the need for increased feed pressures and more complex mass flow controllers to achieve similar propellant mass flow rates

to liquid propellants, poor atomization and burn rates, as well as increased costs compared to both solid and liquid propellants [17,18].

Efforts in characterizing and demonstrating gel propulsion systems include those led by groups from Germany, Israel, and the United States [18]. Notable developments and demonstrations include the successful firing of a TOW missile that utilized a gelled bipropellant propulsion system in 1999 by the now defunct TRW, inc. [18,19]. This system utilized a gelled mono-methyl hydrazine (MMH) fuel with a gelled inhibited red fuming nitric acid (IRFNA) oxidizer and was completed in the Future Missile Technology Integration (FMTI) program supported by the U.S. Army Aviation and Missile Command (AMCOM) [19]. In partnership with the Fraunhofer Institute for Chemical Technology and German based missile company Bayern-Chemie, the German Aerospace Center, DLR, began a developmental program for gel rocket motors (GRM) in the year 2000, and in 2009, successfully launched two demonstrators which are reported to have used gelled monopropellants [20]. The group at Technion in Israel has explored concepts ranging from hypergolic gel propellants to gelled fuel for ramjet engines [18].

1.3. Gel Polymer Electrolytes as Electrically Controlled Propellants

Gel Polymer Electrolytes (GPEs) are ionically conductive materials composed of salts dissolved in a polymer [21]. Because of its ionic transportation qualities, there is potential for a GPE to utilize electrolysis in a similar manner to what has been demonstrated with HAN and ADN ionic liquids, where a sufficient voltage can cause the gel to decompose and ignite in an electrically controlled manner given that the salt component of the GPE is also an oxidizer. In the application of a voltage, the ions that move toward the anode are reduced and subsequently combusted. The use of a GPE in the application of an electrically controlled gel propellant

(ECGP) has potential to circumvent the aforementioned atomization and combustion inefficiencies of gels due to the omission of atomization in the ignition process while maintaining the advantages of gelled propellants. Limited research on the topic of electrically controlled propellants (ECP), primarily as electrically controlled solid propellants (ECSP), has become available in recent years, and will be explored in chapter 2.

1.4. Research Motivation and Scope

The increasing interest in a low-toxicity alternative to hydrazine has led to exciting developments in ionic liquids as monopropellants, including the introduction of electrolytic ignition. The combination of this with the historical interest in gel propulsion systems and the emergence of gel polymer electrolytes presents an opportunity for a novel monopropellant in the form of the electrically controlled gel propellant. This propellant is composed of a GPE that utilizes electrolysis and has potential to address issues experienced in gel combustion.

The primary objective of this research was to explore, characterize, and provide insight to fundamental properties of electrically controlled gel polymer electrolyte monopropellants. A family of five ECGPs was developed, and experiments were completed to characterize the combustion and various material properties of these ECGPs as a function of the ratio of the propellant's oxidizer salts, which was varied between the propellant candidates. Combustion characterization was completed by observing ignition characteristics as a voltage potential is applied to the propellants, followed by a study completed with a select few propellants under varying pressures to describe its burn and extinction properties. Material properties investigated include their mechanical and electrochemical properties, which were determined through

rheology and electrical impedance spectroscopy (EIS) studies, respectively, as well as their thermal decomposition and stability in a thermal characterization study.

2. Review of Relevant Research and Topics

This chapter explores in detail research efforts and developments in topics relating to the present work. Topics include the catalytic and thermal decomposition methods utilized by monopropellants, the electrolytic decomposition of ionic liquid monopropellants, efforts to support the development of gel propulsion systems, recent advances and applications of polymer electrolytes, and finally recent developments in electrically controlled propellants.

2.1. Developments in Ionic Liquid Monopropellants

As mentioned in chapter 1, hydrazine-based monopropellants have made up the most reliable monopropellant options used to date since its introduction in the 1960s [6]. The introduction of the Shell 405 catalyst in 1966 is recognized to have made its use practical in this application possible [5,22]. Hydrazine decomposes into products of ammonia, nitrogen, and hydrogen in a two-step process as described in Equations 2.1 and 2.2 [23].

$$N_2H_4 \rightarrow \frac{4}{3}NH_3 + \frac{1}{3}N_2 \quad \textbf{(2.1)}$$

$$NH_3 \rightarrow (1-x)NH_3 + \frac{1}{2}N_2 + \frac{3}{2}xH_2 \quad \textbf{(2.2)}$$

Here, *x* represents the dissociation of ammonia, which was found to play a role in the performance of the monopropellant [5,23]. The increase in dissociation of ammonia is found to have a negative effect on the monopropellant's I_{sp} and flame temperature, and early in the catalyst's development, Price and Evans state that Shell 405 would generally lead to more

dissociation [5]. Advances since then have found ways to improve upon this feature. However, the health and safety hazards due to hydrazine's high vapor pressure and toxicity as well as the associated costs in the use of hydrazine and its derivatives, such as monomethyl hydrazine (MMH) and unsymmetrical dimethyl hydrazine (UDMH), have motivated a global search for so-called green monopropellant alternatives, with some programs including joint efforts across multiple nations [6,7,10,11,24]. Ionic liquid monopropellants that utilize ADN and HAN have been suggested as the most suitable alternatives, with low toxicity, performance exceeding that of hydrazine, preferable physical qualities such as low freezing points, and their quickly developing technology readiness over the course of the past two decades [6,7,11,25]. As previously stated, Current applications that employ monopropellants typically utilize catalytic or thermal ignition methods, however, the development of IL monopropellants present an opportunity for electrolytic ignition methods to be explored. The following sections will discuss efforts in the development of ADN and HAN IL monopropellants, including studies completed on these ignition methods.

2.1.1. Catalytic and Thermal Methods in IL Monopropellants

The Shell 405 iridium-alumina catalyst is regarded to be exceptionally durable in its use with hydrazine, as several studies have shown low degradation in its surface area over exposure times on the order of an hour or longer and provides quick ignition at cold temperature [5,24]. A common challenge associated with the use of catalysts in most monopropellant formulations is its ability to withstand high temperatures without significant loss of surface area, calling into question the durability and lifespan of possible applications, and provide the necessary energy to ignite the monopropellant without the need for high preheat temperatures [25]. Typical

temperature stability limits of catalysts are around 1200°C, which the combustion of HAN and ADN solutions easily exceed, while hydrazine presents a special case with its low combustion temperature at around 900°C [9,11,13,26]. Iridium catalysts are among those most commonly used, and a study conducted by Amrousse, Katsumi, et. al. using a HAN based ionic liquid showed that these catalysts experience their share of issues when exposed to high temperatures. Oxidation, loss of surface area, and sintering during the reaction were identified as problems that resulted in the catalyst's deactivation, leading to increased reaction times [27]. Work to find new catalysts and understand catalytic compatibility with HAN and ADN based solutions have been among the major steps in developing these monopropellants. Courthéoux et. al. acknowledged that the most important aspects to consider when developing new catalysts include its ability to trigger the monopropellant at low initial temperatures, preferably at or below room temperature; the reduction of the ignition delay; stability in high temperatures; and the limitation of combustion by-products such as nitrogen oxides [28].

In 2005, Courthéoux et. al. conducted an examination to compare thermal and catalytic decomposition processes of solutions consisting of HAN diluted by varying amounts of water using a platinum activation metal and silica-alumina support catalyst. They found that the thermal decomposition onset of their HAN solutions occurred only when water had been entirely evaporated, in excess of 100°C, but with the use of their catalyst, the decomposition process could be triggered at temperatures approaching room temperature, even with the presence of water. They also noted that, to achieve improved performance of the monopropellant, fuels such as glycine or methanol can be added [28]. Amrousse, Hori, et. al. later conducted a similar study to compare the catalytic and thermal ignition responses of both HAN and ADN based monopropellants using iridium and copper oxide activation metals supported by a lanthanum-

oxide-doped alumina bed as catalysts. Their findings supported the conclusions of Courthéoux's study, showing that the presence of water in both led to high thermal decomposition temperatures, including 152°C for their HAN formulation and 116°C for their ADN formulation. With the appropriate use of their catalysts, the decomposition temperature decreased to 47°C for the HAN solution and to 51°C for the ADN solution [25].

A novel form of catalyst development for possible aerospace applications was examined in studies out of Europe centered around the RHEFORM program, which was a joint effort between multiple nations that focused on the replacement of hydrazine with ADN based ILs between 2015 and 2017. This program introduced and investigated the 3D printing of ceramic monolithic catalyst supports for use in thrusters in an effort to achieve high fidelity, porous geometries with increased surface areas that had better temperature stability. The general motivation was to decrease the need for exotic materials that are otherwise limited by International Traffic in Arms Regulations (ITAR) [26]. A continuation of this program known as the Horizon H2020 RHEFORM project was completed with a similar goal, however, they focused on the formulation of propellant and catalyst compositions that reduce combustion temperatures so that ITAR-free materials could be utilized [29]. One study within this program was conducted by Maleix et. al., who worked to verify the fidelity of 3D printed monolithic catalyst supports using Scanning Electron Microscopy (SEM) as well as to determine the potential for these monoliths and their integrity in decomposition tests with FLP-106 and LMP-103S monopropellants. The results showed that specific features in surface area of the monolithic catalyst could be maintained for an extended period at 1200°C and in short exposure to 1500°C temperatures, showing that degradation issues in catalysts could be improved [30].

At the DLR, Wilhelm et. al. looked further into the application of the thermal decomposition of the ADN based FLP-106 and LMP-103S monopropellants to observe their thermal ignition behavior. Here, the group developed two demonstrators to conduct preliminary ignition experiments using a pilot flame igniter as well as a glow plug igniter, the latter of which may be capable of achieving multi-start operation. In support of previously mentioned conclusions regarding the thermal decomposition of these ionic liquid solutions, it was shown that the evaporation of the water present was necessary before any decomposition or ignition could take place. It was deduced that the heat transfer from the ignition source to the propellant was a driver in this ignition issue, as an effective mode of heat transfer would instigate the necessary evaporation quicker and allow for a shorter ignition delay of the propellant [31].

Ignition of IL propellants by thermal means requires a significant amount of energy to compensate for the presence of water [25,28,31]. While ongoing efforts to develop effective catalysts for IL monopropellants are progressing with promising results and innovations, such as consistent catalysis at preheat temperatures that are approaching, but not quite reaching room temperature, and methods that improve catalyst lifespan issues, the ionic nature of the solutions have led to research efforts that explore electrolytic decomposition and ignition methods [32].

2.1.2. Electrolytic Methods in IL Monopropellants

Interests in electrolytic ignition in monopropellants have been a fairly recent development. However, a report published by a group at the U.S. Air Force Rocket Propulsion Laboratory dating back to the 1970s presented work completed to characterize the ignition delay of hydrazine using this method. Here, the group was able to demonstrate repeated electrolytic ignitions of the monopropellant [33]. While little development and research in electrolytic

ignition has been made public since this first proposal, some research has demonstrated the use of this mechanism to limited extents. In 1989, Vosen demonstrated the use of a voltage to ignite a HAN based solution in a strand burner, and in 1993, Carleton et. al. used electrolysis to assist in the thermal decomposition of HAN, noting that this led to quicker laser ignition than a sample that did not have the same exposure [15,34,35].

The use of electrolysis, especially in micro-propulsion applications where thermal management is difficult to control, has garnered interest due to its perceived efficiency in transferring energy directly to the propellant to achieve ignition as opposed to traditional means of catalysis and thermolysis [15,36]. In the micro-scale application, heat and energy loss become significantly more detrimental to the system due to a high surface-to-volume ratio that exists between the propellant and the thruster [36,37]. Risha et. al. describes the potential benefits of electrolytic ignition in small-scale applications as lower ignition temperatures; reduced power requirements; better thermal and power management; enhanced system durability, reliability, and reusability; and reduced costs [15].

In more recent endeavors, Risha et. al. utilized a titanium microfin electrode in the HAN solution, XM-46, applying voltages up to 26V. They observed a rise in temperature to the point of gasification of the solution, which agreed with the known decomposition temperature of HAN at 115°C. The group also concluded that, while temperature was independent of the voltage magnitude, time to gasification was not, as time to gasification decreased drastically from 160 seconds to only a few seconds when the voltage increased from 7V to 12V [15]. In 2015, Khare et. al. conducted a similar study on the ignition delay of a HAN-water solution. However, this group characterized the solution's ignition delay over varying propellant volumes subjected to the electric potential, varying concentrations of HAN, and varying electrical currents at a fixed

voltage. Electrolysis was found to be promoted by decreasing the volume of the propellant, which led to an increase in current density, while decreasing the concentration of HAN was found to inhibit the process as the available ions in the solution decreased. The increasing current led to significant decreases in ignition delay, which they described as a power-law function [38]. Wu and Yetter explained that the electrolysis of HAN occurs at a lower activation energy than its thermal decomposition, which relies only on a proton transfer mechanism. In its electrolysis, reactions that occur at the anode and cathode compete with one another as well as the proton transfer reaction to accelerate decomposition of the solution [36]. In their study of HAN, Wu and Yetter developed and tested a thruster that utilized electrolysis to characterize thrust performance and describe the effects of voltage magnitude on ignition delay. Tests were conducted at 20V, 40V, and 60V, with the middle voltage resulting in the shortest ignition delay. The propellant's complete ignition was accompanied by a large spike in current, which is indicative of a quick reaction from decomposition to ignition [36]. This suggests that, for some formulations at least, an optimal voltage range can exist and surpassing it will not continue to decrease the ignition delay.

Koh et. al. conducted a study to observe the effects of electrode material on the, made of copper or aluminum, continuously oxidized in the solution when powered, leading to an increase in electron donation which enhanced this process. This was especially noted in the use of the copper electrodes, as the solution would turn bluish near the anode as Cu^{2+} ions were produced. An inert electrode made of carbon was not found to directly instigate an electrolytic reaction, as the electrons were confined to travel across layers of the electrode as opposed to across the medium from one electrode to another, leading to little observed changes in temperature while power was supplied. However, when the power supplied to these carbon electrodes was turned

off, the HAN solution was observed to increase drastically in temperature, in what they believed to be an autocatalytic event [39].

In the study of electrolysis with ADN-based solutions, many of the same examinations were completed. A study completed by Lei Li et. al. observed the electrical ignition and combustion characteristics of FLP-106 and LMP-103S as a function of voltage and droplet size. As one might expect, it was found that increasing the droplet size drastically increased the fluctuation in both combustion efficiency and duration. It was also concluded that the increase in voltage decreased ignition delay and combustion duration in these droplets. The ignition delay as a function of voltage was found to be a nonlinear relationship as well [40]. In a similar study conducted by this group with additional personnel, the electrolytic combustion of an ADN solution was characterized as a function of voltage in three different gas environments, including under argon, air, and nitrous oxide. The group reported combustion pressure; current, ignition energy, and total energy; and the mole fractions of reaction products resulting from the combustion process. The performance aspects of these experiments were independent of the atmospheric gas used, as the propellant utilizes its stored oxidizer to combust, however, the peak combustion pressure in the presence of nitrous oxide was found to be almost twice that of argon. The concentration of nitrous oxide as a product of combustion was found to increase with voltage, while the concentration of carbon monoxide was found to decrease. It was once again observed that the increase in voltage decreased the ignition delay of the propellant as well [41].

Rahman et. al, tested the electrolytic combustion of FLP-103, an ADN-based monopropellant similar to the previously mentioned FLP-106, in an open chamber as well as a micro-electrical-mechanical system (MEMS) thruster to characterize its power consumption. The group utilized copper electrodes in their configuration and primarily noticed reactions occurring along the

cathode owing to the donation of electrons as the copper oxidized. The electrolysis was first detailed in the open chamber experiments, where the production of bubbles as power was supplied was used as the metric to find an optimum power consumption. A test of various power inputs showed that a setting of 80V at 0.1A (8W of power) generated bubbles the quickest, whereas a setting of 5V and 2.5A (12W of power) was the slowest. In the MEMS thruster, multiple flowrates were tested across multiple power inputs at a fixed applied current. As voltage increased at the lowest flowrate of 40 $\mu L \cdot min^{-1}$, the decomposition and combustion became more complete, as only a plume of exhaust gas was produced from the nozzle. The higher flowrates produced both a plume as well as undecomposed propellant [37].

Efforts completed to advance the understanding and applications of electrolysis for use in IL monopropellants have commonly demonstrated the dependence of decomposition and ignition on the applied voltage and volume. The exploration of electrolysis in this manner has led to interest in electrically controlled propellants that utilize polymer electrolytes, which will be noted upon further in this chapter.

2.2. Gel Polymer Electrolytes

Polymer Electrolytes (PE) emerged in the 1970s as materials composed of a salt-polymer complex that forms as a result of the interaction between oxygen in the polymer and the cations in the salt molecules. This interaction causes the salt to dissolve and breakdown into its cation and anion constituents within the medium. The ability for these ions to move freely across the medium gives the material its ionic conductivity, which varies depending on the type of PE; a couple to note include the solid polymer electrolyte (SPE) and the gel polymer electrolyte (GPE) [21].

GPEs differ from SPEs as they use a plasticizer or gelled polymer for the matrix as opposed to a solid polymer to become a gel or plastisol. This gelled or liquid medium driving its ionic transportation properties [21,42]. The complex can be created by heating and stirring together the plasticizer and salt, either with or without a solvent. The physical and electrochemical properties of GPEs depend on the plasticizer used, which may be low molecular weight organic polymers, organic solvents, or ionic liquids [21]. Polyethylene Glycol (PEG), which is a low molecular weight Polyethylene Oxide (PEO), is commonly used as the polymer in GPEs due to its ability to be readily complexed with lithium salts [43-45]. Common uses for PEs are focused on reusable, reliable, and safe power cells, and capacitors [21,42,45-47].

Rechargeable lithium-ion batteries use an anode and cathode through which the PE is charged or discharged. Upon the application of a voltage, or in the charge of the PE, the cations move from the cathode to the anode, while the anions move in the opposite direction. When the PE is discharged, this is reversed, and the electrolyte releases a voltage [21]. The development of GPEs for the use in lithium-ion batteries, which typically utilize a liquid electrolyte, is motivated by safety and reliability issues seen in the current state. Such issues include the possibilities of leakage, internal shorting, and combustible reaction products [42,45]. While SPEs are sought after for their inherent safety and energy density, their ionic conductivities are too low in their current configuration to constitute practical use. GPEs are more readily applicable due their increased ionic conductivity as well as their displayed combination of benefits derived from both solid polymer and liquid electrolytes, including preferable mechanical strength and flexibility, thermal stability, good compatibility with electrodes, among others [45,47].

W. Li et. al. completed a study to characterize the electrochemical and thermal properties of a PEO-based GPE that utilized lithium perchlorate (LP) prepared via in situ polymerization. These

properties were compared to those of a commercial separator saturated in a liquid electrolyte, and results showed that the prepared GPE improved upon the thermal stability and maintained the same level of electrochemical performance [45]. Polymer electrolytes have also gained much interest in use as capacitors and supercapacitors due to their high electrical energy density and ionic conductivity [46]. Sudhakar and Selvakumar described the use of an LP-doped chitosan and starch polymer blend for potential use as a supercapacitor, completing various electrochemical experiments to find that their compositions performed with high conductivity, energy density, and capacitance [46].

The research described in this thesis was interested in utilizing a GPE's ionic capabilities alongside its composition of a polymer and oxidizer salt, such as LP, to detail its potential application as a monopropellant that utilizes electrolysis as an ignition method.

2.3. Efforts in Gel Propulsion

As mentioned in chapter 1, gelled propellants have been of interest for quite some time due to their favorable safety qualities and comparable performance to some liquid propellants [17,18,20]. Gelled bipropellants have been demonstrated and present a special opportunity in hypergolic configurations, as catalysts can be suspended within the matrix of the gel to facilitate combustion [19,48]. Research efforts primarily focus on improving the combustion, atomization, and injection difficulties with gelled propellants and fuels. [17,18,49].

Various studies have resulted in well described characteristics of the combustion of gelled fuels [17,49-51]. A study completed by Nachmoni and Natan in the late 1990s to describe the combustion characteristics of gelled JP-5 fuel with organic gellants showed that the combustion of their prepared gel follows the d^2-law for droplet evaporation and combustion, which linearly

relates the burn time of the droplet, which is given as t_b, to its original square diameter, d_o^2, by the burn rate coefficient K. This relationship is depicted in Equations 2.3 – 2.5 [49,50].

$$d_d^2(t) = d_0^2 - Kt \quad \textbf{(2.3)}$$

$$K = \frac{8D\rho_g}{\rho_d}\ln(1 + B) \quad \textbf{(2.4)}$$

$$t_b = \frac{d_0^2}{K} \quad \textbf{(2.5)}$$

Here, ρ_d is the droplet density, ρ_g is the density of the gas as a result of the evaporation or combustion, while D is the oxygen diffusivity, and finally, B is the Spalding transfer number. It is of note that the burn rate coefficient is only constant in the presence of a steady-state temperature at the surface of the droplet, providing [50].

Nachmoni and Natan, however, observed that the addition of a gellant and further increase in its content increased the heat of vaporization for the fuel, leading to decreased burning rates and increased burn times [49]. Arnold and Anderson conducted a similar examination, but with JP-8 fuel gelled with fumed silica, which is an inorganic gellant. In their study, it was determined that increasing amounts of this inorganic gellant resulted in a deviation from the d^2-law. It was also observed that droplets with increased silica content had an accumulation of unburned silica present, which resulted in both a nonuniformity in temperature across the volume of the droplet and combustion instability [50]. This work was further supported by a more recent study

completed by Cao et. al. on droplets of kerosene fuel gelled with fumed silica. Here, the combustion of the fuel droplets is described in a few stages. Early in the burning process, a stiff silica shell forms to encapsulate the fuel, which then shrinks and is shed as the fuel vaporizes. As the internal pressure increases, the shell fractures and the droplet combusts. This group similarly concludes that the d^2-law is followed with low concentrations of the silica gellant, but the deviation from this law increases with the silica content, possibly due to the formation of the rigid structures that remain unburned [51].

The atomization of gelled propellants with the use of impinging jet injectors to observe morphology under various conditions has been studied for some time as well [17,52,53]. A recent study completed by Guan et. al. utilized an ADN-based gelled propellant with a swirl-nozzle injector configuration to study the effects of injection pressure on nozzle mass flow rate, spray cone angle, breakup length, and the Sauter mean diameter (SMD) as a means to characterize the propellant's effective atomization. It was observed that increasing the injection pressure resulted in rapid increase in spray cone angle across the low-pressure range but stabilized at higher pressures. The rate at which the SMD decreased over the low pressures was fairly rapid as well and slowed with the higher pressures [53].

Various difficulties in the combustion and atomization of gelled propellants have remained as limiting steps in realizing their application in practical use. An alternative that has potential to circumvent these issues has developed over recent years from the evolving interest and research completed on both electrolytic ignition methods of monopropellants and polymer electrolytes. Due to their ionic conductivity and use of a polymer, PEs display potential as ECPs in either their gel or solid states.

2.4. Electrically Controlled Propellants

Polymer electrolytes display a unique combination of composition and ionic properties that, when saturated with an oxidizer salt, would allow for electrolytic combustion to occur in an electrically controlled manner. This includes decomposition and ignition with the application of a voltage potential, a variable energy output and burn rate dependent on the voltage magnitude, and extinguishment upon removal of the voltage [54,55]. Recent investigations have commonly focused on the use of a solid polymer electrolyte to achieve this, however, some efforts have incorporated gels as well. Researchers have employed ionic liquids, such as HAN, or ionic salts, such as LP, to provide the PE with its ionic conductivity. Polymers typically used are polyvinyl alcohol (PVA) or PEO [55,56].

In 2007, Khoruzhii et. al. showed that an ammonium nitrate (AN) based solid propellant burned under the application of a voltage, and that the burn rate was dependent on this voltage. It was concluded that a liquid phase must be present to drive the ionic conductivity which led to the combustion of the propellant, while the condensed or solid phase had little ionic conductivity [57]. Gobin et. al. completed a similar investigation in 2019 with AN and LP solid oxidizers, demonstrating the dependence of their decomposition on applied voltage as well. Here, it was shown that the presence of a melt layer was required for the voltage to alter the regression rate of the oxidizers, reaffirming Khoruzhii's findings [58]. The exploration of the effects of an electrical stimulus on the decomposition of oxidizers and propellants have led to an interest in developing ECPs.

Efforts using HAN and PVA based ECSPs have been reported to demonstrate poor thermal stability and electrical controllability [55,59]. A study by He, Xia, et. al. was completed to explore options to improve up this, characterizing the thermal stability as well as burn rate as a

function of applied voltage of an ECSP utilizing LP and PVA. Their results were compared to a prepared HAN, water, PVA, and aluminum ECSP, and found that their ECSP was more thermally stable, with a decomposition temperature 62°C higher. The dependence of burn rate on voltage was demonstrated as well, showing that an increase of applied voltage from 80V to 400V resulted in an increase in burn rate by about eight times [55]. Similarly, Ma et. al. explored the effects of oxidizer selection on thermal stability by determining thermal decomposition temperatures of three ECSPs. The first utilized only ADN in its oxidizer, the second utilized AN, and the last contained a mixture of the two at a ratio of one part AN to three parts ADN. Their findings showed that the propellant composed of mixed oxidizer achieved the highest thermal decomposition temperature at 223°C, which exceeds the decomposition temperature of the propellant composed of only ADN by about 28°C [54].

Baird et. al. has characterized the electrolytic mechanisms that lead to the combustion of a HAN and PVA plastisol, detailing the oxidation-reduction processes that occurred at the anode and cathode which lead to the propellant's combustion. The oxidation of the nitrate anion at the anode, which produces a highly reactive oxygen radical that is absent of two electrons, is believed to cause combustion [60]. Baird and Frederick further expound upon the previous study by exploring the thermochemistry in the combustion of this plastisol, creating an electrolytic model to describe possible combustion products. By considering the typical products of HAN-PVA combustion, which include carbon monoxide, water, nitrogen, and hydrogen, along with different proposed oxidizing and reducing agents in the electrolytic reaction that occurs along the electrodes, they were able to determine the theoretical heat of combustion [61].

Studies conducted by Gobin et. al. has observed the electrolytic combustion of GPE monopropellants with varying amounts of polymer. A 1:1 ratio of LP and AP oxidizer salts were

utilized with PEG. The study determined that the polymer content had substantial effects on the material and combustion properties of the gels. This study demonstrated that competing processes exist in their ignition and combustion; while it is believed that the mechanisms are electrolytically dominant, an increase in resistivity would lead to higher rates of ohmic heating. At some point, the competition between these processes begins to accelerate the decomposition and ignition of the gels. [56]. This phenomenon appears in the study detailed by this thesis and will be further discussed in chapter 5.

Efforts to explore ECPs are relatively new yet are rapidly progressing with the development and characterization of various compositions. Existing studies have often demonstrated ignition by electrochemical means, throttling by varying the applied voltage, and extinguishment in terminating the applied voltage. The research detailed in this thesis was focused on continuing work completed by Gobin et. al. and further explore the characteristics of gel polymer electrolytes as an ECGP.

3. Experimental Methods

This chapter discusses the process of selecting and preparing the candidates that became the family of electrically controlled gel polymer electrolyte monopropellants studied. Experiments conducted to characterize various material properties as well as combustion properties at both atmospheric and elevated pressures of the monopropellants are introduced.

3.1. Monopropellant Selection

The family of monopropellants utilized the oxidizer salts of ACS grade lithium perchlorate, sourced from Thermo Fisher Scientific with a minimum purity of 95%, and ammonium perchlorate (AP) with a stated particle size of 200 μm, sourced from Pyro Chem Source. The ionically conductive polymer used was polyethylene glycol (PEG) with a molecular weight of 400 $g \cdot mol^{-1}$ sourced from Sigma-Aldrich. Acetonitrile (ACN) with a minimum purity of 99.9%, also sourced from Thermo Fisher Scientific, was used as the solvent in the preparation of samples. This was the chosen solvent as it is historically common to use in Lithium-PEO polymer electrolytes, as PEO readily absorbs acetonitrile [62,63]. LP was used in conjunction with PEG due to the extensive research available on these components in GPE applications, which describe the ability for PEG to be readily complexed with lithium salts, as well as the work demonstrated in ECP applications [43-45,56,58]. The addition of AP was for the purpose of tailoring the behavior of the propellants as AP is a well-known oxidizer with predictable characteristics. The oxidizers used are depicted in Figure 3.1.

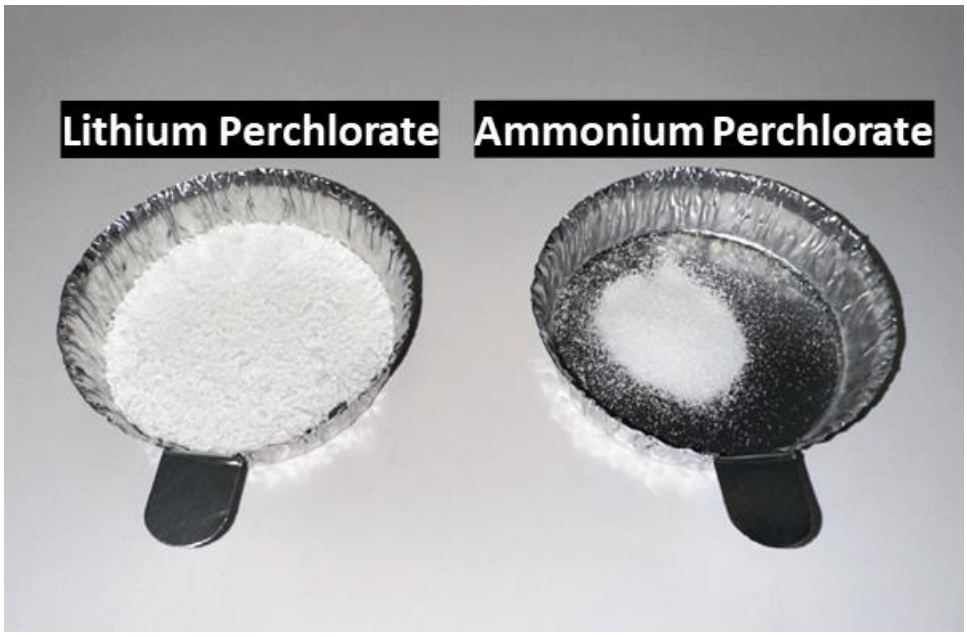

Figure 3.1: Lithium perchlorate and ammonium perchlorate oxidizer salts used in experimentation.

For safety and storage reasons, as well as the monopropellants' ability to be electrically controlled, it was provided that a flame should not sustain once the ignition source was removed. This criterion was observed early in the selection process of the monopropellants. Possible formulations of the gels were thermally ignited with a torch and, upon removal of the flame, its ability to extinguish on its own was determined. An early propellant candidate that sustained a flame had an oxidizer composition of 50% AP and 50% LP as well as a polymer to oxidizer ratio of 1:3. This ratio of oxidizer components was selected as the upper limit of what would be studied. Once an upper limit of AP content was established, the concentrations of the constituents in the monopropellants were determined based on theoretical performance criteria. NASA's Chemical Equilibrium with Applications program (CEA) was used to calculate these performance parameters, which included flame temperature and vacuum specific impulse (I_{vac}) [64]. For each

of the following CEA calculations, the equilibrium rocket problem was used with an assigned chamber pressure of 0.689 MPa and a supersonic area ratio of 100.

CEA was first used to find the polymer to oxidizer ratio at which the thermochemical performance of the propellant is maximized. This is shown in Figure 3.2 below, which depicts the performance of propellants composed of LP and PEG as well as AP and PEG as a function of polymer weight percent. It was found that the LP-PEG propellant had its thermochemical peak at 25% polymer weight, while that of the AP-PEG propellant occurred at 15% polymer weight. Due to the study's focus on electric controllability and use of AP as an energetic supplement, a 1:4 polymer to oxidizer ratio was selected to reflect the thermochemical peak found for the LP-PEG propellant.

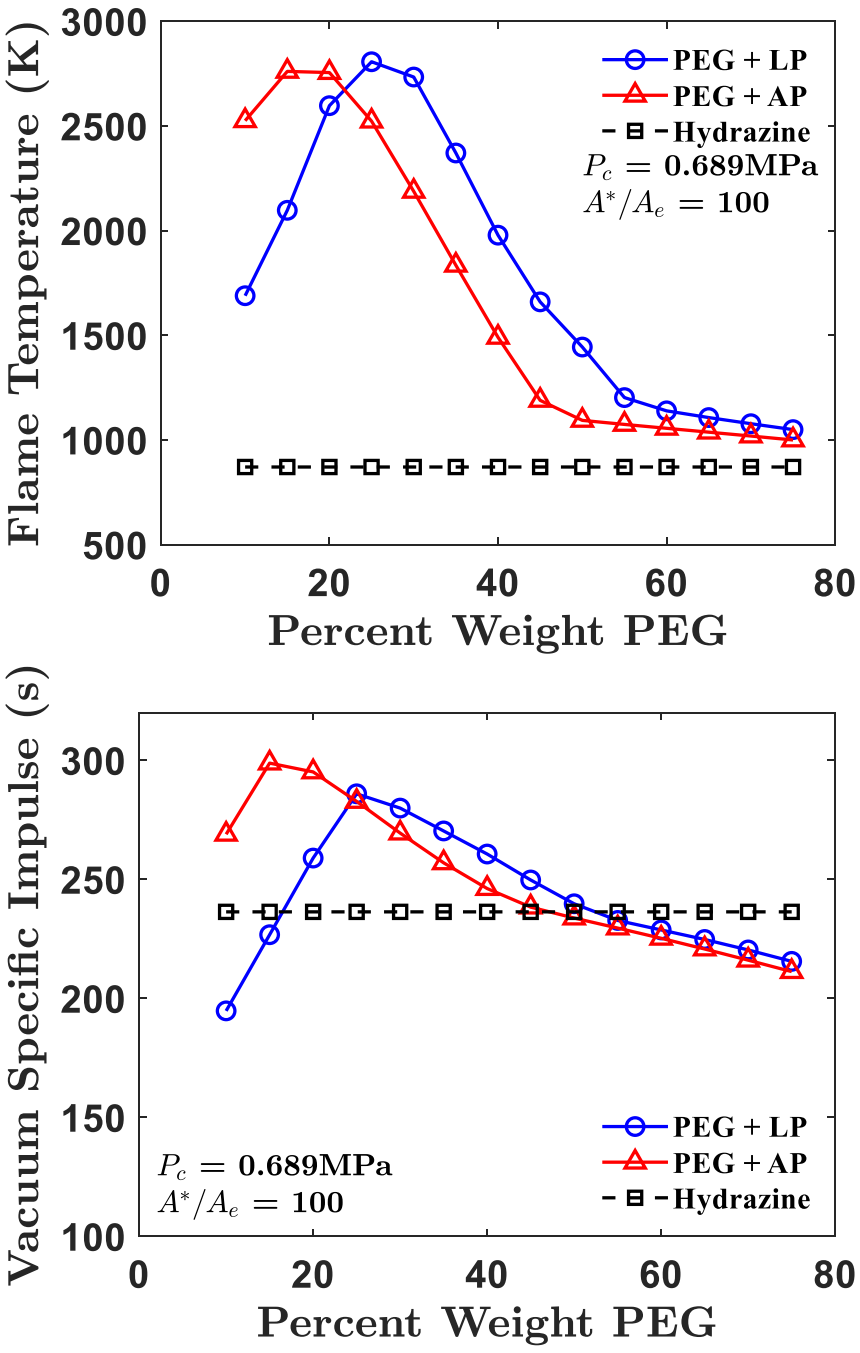

Figure 3.2: Polymer weight percent vs. flame temperature (top) and vacuum specific (bottom) impulse for PEG+LP and PEG+AP compositions.

CEA was next used to show the effects of varying the oxidizer content on the flame temperature and vacuum specific impulse and ultimately select the composition of monopropellant candidates to be further studied. Theoretical calculations of these parameters were found as a function of AP weight percent at the selected polymer to oxidizer ratio, with LP making up the remaining oxidizer mass. Depicted in Figure 3.3 are results of these calculations compared to theoretical values for the hydrazine monopropellant, which were also found using CEA at the same conditions. It is shown that there is little variation in performance for the GPE monopropellant as oxidizer content is adjusted. Thus, a baseline monopropellant composed only of LP and PEG as well as four monopropellants with increasing AP content were selected to have their material and combustion properties characterized, and are represented in Figure 3.3 as vertical, black-dashed lines. Table 3.1 details the composition of these selected candidates. Because this work is a continuation of prior research completed to explore characteristics of ECGPs by Bradley Gobin, et. al., the naming convention of the gels studied in this work is seen to begin at number fou

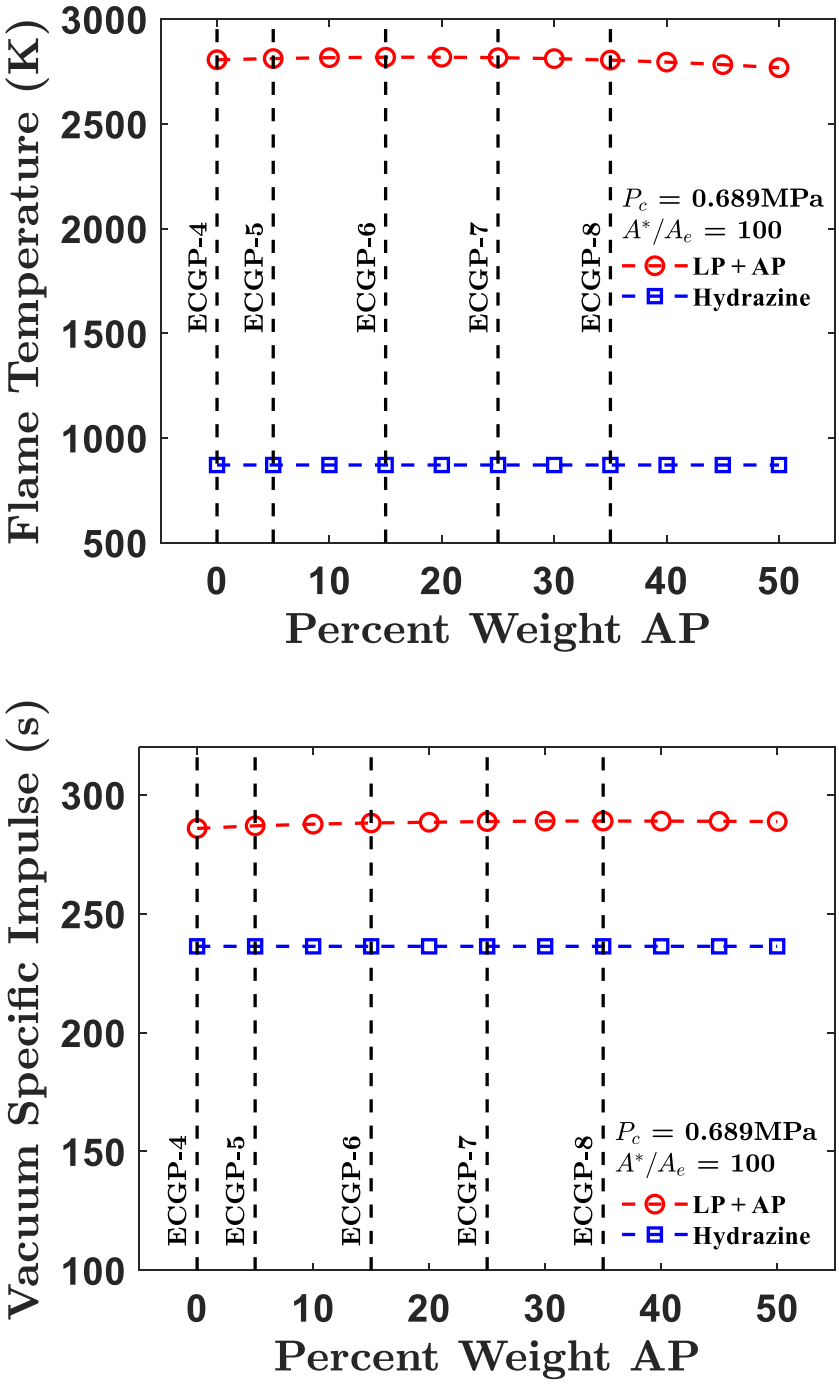

Figure 3.3: AP weight percent of total oxidizer vs. flame temperature (top) and vacuum specific impulse (bottom) at 25% weight polymer.

Table 3.1: Compositions of gel propellant candidates.

Candidate Name	%wt PEG	%wt LP	%wt AP
ECGP-4	25.00	75.00	0.00
ECGP-5	25.00	71.25	3.75
ECGP-6	25.00	63.75	11.25
ECGP-7	25.00	56.25	18.75
ECGP-8	25.00	48.75	26.25

3.2. Monopropellant Sample Preparation

The monopropellants were prepared in lab-grade borosilicate beakers ranging in size from 50 mL to 200 mL depending on the amount of sample to be manufactured. The polymer was first pipetted directly into the sample beaker atop a scale. Solvent was then pipetted into the beaker under a fume hood, in an amount equal to the total mass of the propellant sample, and this mixture was covered with aluminum foil to prevent the evaporation of the solvent. A stir bar was added to the beaker, which was then allowed to stir on a heated stir plate for up to an hour, allowing the polymer to completely dissolve into a solution. The oxidizer salts were weighed separately in weigh boats and added to the polymer solution in multiple additions to improve consistency of dissolving. This mixture was stirred while covered and heated anywhere from one to multiple days, typically in the range of 40°C to 50°C, until the LP particles were sufficiently dissolved. is believed that the larger AP particles, however, do not fully dissolve and are instead left suspended in the gel matrix to some extent. The mixture was then stirred uncovered to allow

the solvent to evaporate and the mixture to thicken, again over the course of a few days. Once too thick to stir, the stir bar was removed, and the mixture was placed in a vacuum chamber to dry further. The monopropellant sample was considered dry after three days in the vacuum chamber, over which the sample was frequently stirred by hand and placed back under the running vacuum until bubbles in the sample ceased. It was then stored in the vacuum chamber until experiments were conducted to avoid the absorption of atmospheric moisture. The final monopropellant was an opaque homogeneous material with consistency similar to petroleum jelly. The time period of the entire manufacturing process was dependent on the amount of sample produced, but typically spanned a week. Figure 3.4 depicts the manufacturing steps up to the final, dried monopropellant that is ready for experimentation.

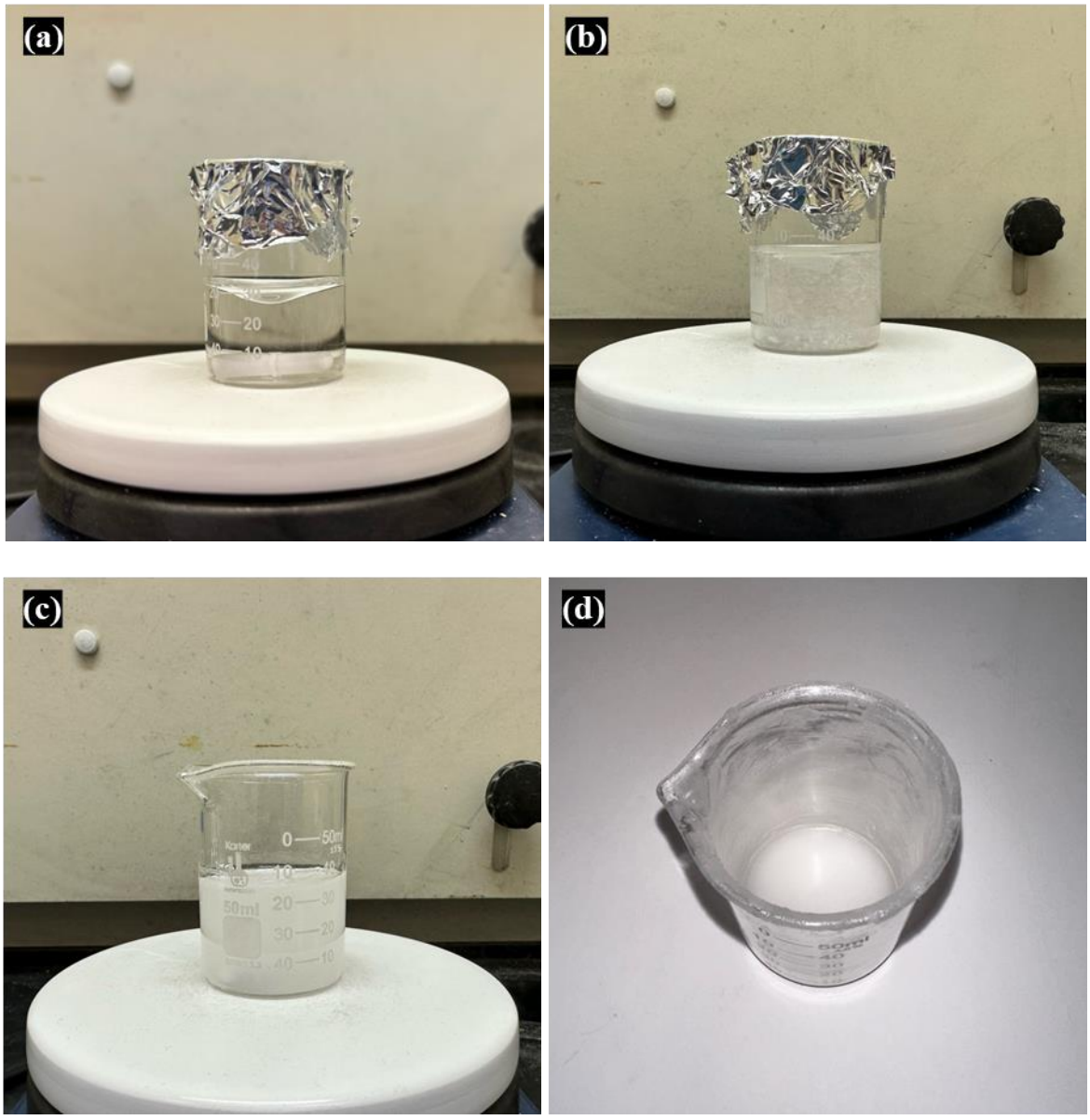

Figure 3.4: Manufacturing steps of ECGP, including (a) the polymer-solvent solution, (b) the addition of oxidizer salts, (c) the solution with dissolved oxidizer salts, and (d) the final gel product of ECGP-6.

3.3. Combustion Experiments

Experiments were completed to characterize combustion aspects of the gel monopropellants. First, their ignition and controllability using a range of applied voltages at atmospheric

conditions was demonstrated. A study to examine the combustion behavior of a select few monopropellant candidates under pressure was then completed, consisting of the determination of their pressure deflagration limits (PDL) and their respective burn rates at their respective PDL.

3.3.1. Ignition Delay Using an Applied Voltage

The experimental investigation of the ignition of the ECGPs with an applied voltage as a function of oxidizer content and electrode spacing was completed using high-speed cinematography and a testing apparatus developed by Gobin et. al. [56]. In this apparatus, which is depicted in detail in Figure 3.5, the gel monopropellants were fed into the channel of an alumina ceramic test block by a stainless-steel syringe with an alumina nozzle that was loaded into a Harvard Apparatus PHD Ultra syringe pump. The channel was lined with two copper plate electrodes on either side which applied voltage across the gel when contact was sustained with both. The electrodes measured 0.635 cm in width and were soldered to copper wires that connected them with an XP HPT5K0-L DC power supply, which was controlled with the XP Power Supply Manager software. The assembly was placed on top of a quartz window that was situated in a flame-retardant fiberglass-epoxy test stand with a mirror situated underneath for a Vision Research Phantom VEO 7.10L high-speed camera to capture video. With the continuous application of sufficient voltage to the monopropellant, decomposition and ignition followed by a sustained flame was achieved and contained within the ceramic test block in view of the high-speed camera. The use of a ceramic test block to house the electrodes as well as the ceramic syringe nozzle was to ensure that the accidental electrification of nearby conductive material, such as the syringe pump, was avoided. These experiments were conducted in a fume hood, with the testing environment photographed in Figure 3.6.

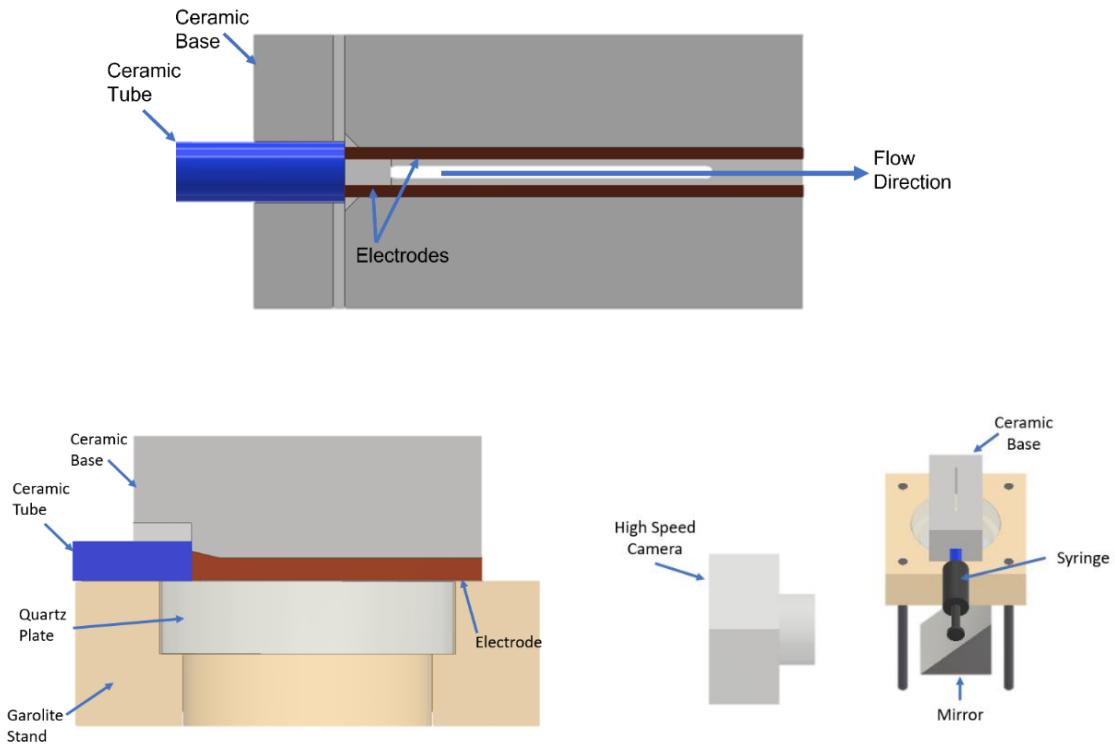

Figure 3.5: Detailed apparatus set up [56], depicting Bottom-Up View (top), Side-Half-Section View (left), and the Experimental Stand Assembly (right)

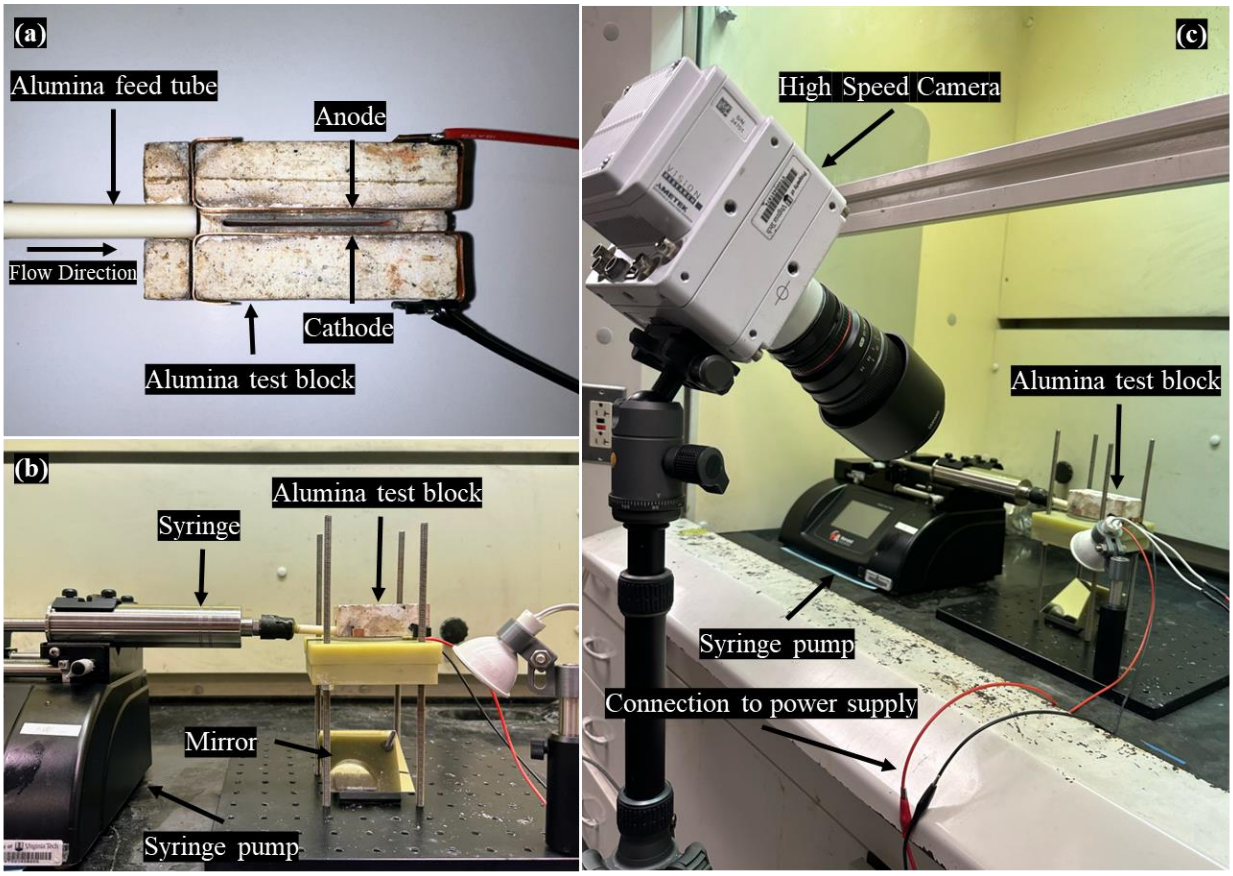

Figure 3.6: A detailed display of the experiment environment, including (a) the electrode and alumina block configuration, (b) the front view of the experimental test stand inside the fume hood, and (c) a view including the high-speed camera configuration.

In these experiments, the ignition delay of each monopropellant was characterized over a voltage range of 120V to 180V in increments of 20V with an electrode spacing of 0.635 cm based on the work completed by Gobin et. al. [56]. This was also completed for ECGP-4 using an electrode spacing of 0.318 cm to observe any dependence of ignition delay on the distance between electrodes, for which a ceramic block with a channel width of 0.318 cm was used. At least three tests were completed at every data point for each monopropellant. The ignition delay was considered to be the time between the gel's initial contact with the powered electrodes and the

first sign of the presence of a flame. Once a flame developed at the gel front, the power supply was turned off, extinguishing the propellant. This process was captured at a rate of 250 frames per second and a resolution of 512 pixels by 512 pixels with the high-speed camera. With knowledge of the respective frames of these events and the sample frame rate of the camera, the ignition delay was determined.

3.3.2. Pressurized Combustion

ECGP-4, ECGP-6, and ECGP-8 were selected to be studied under pressure in an optically accessible strand burner with a nitrogen purge. This was done to determine the respective pressure deflagration limit of each selected propellant, which is the minimum pressure required to sustain the combustion of a propellant [65]. This was an iterative process involving the repeated ignition of the propellant at varying pressures until the threshold at which it bordered a sustained flame and extinction was found. The average regression rate of each of the gels in question at their PDL over three experiments each was determined as well. These parameters are important to consider when determining the operating pressure of the propellant so as to avoid unintentional deflagration when not in use [65].

Samples of the selected propellants were placed in homemade sample carriers composed of a quartz tube with one end open and the other end epoxied to a 3D printed closure. This is visualized in Figure 3.7. A homemade AP solid propellant was utilized as an igniter, which was placed at the open end of the sample carrier in contact with the gel. The solid propellant was composed of 65% by mass AP with a stated particle size of 200 microns and 10% AP with a stated particle size of 90 microns, both sourced from Pyro Chem Source; 17% hydroxyl-terminated polybutadiene (HTPB), with R-45 polymer and Methylene Diphenyl Diisocyanate

(MDI) curative sourced from RCS Rocket Motor Components, inc.; and 8% spherical aluminum powder sourced from Valimet, inc. with a stated minimum purity of 99.7% and a particle size determined to be between 600 nm and 2000 nm [66]. A nichrome wire which was laid atop the gel was used as an ignition source via a power supply. The tube assembly was held in the strand burner by a flame-retardant fiberglass-epoxy composite base, and the configuration is detailed in the schematic shown in Figure 3.8.

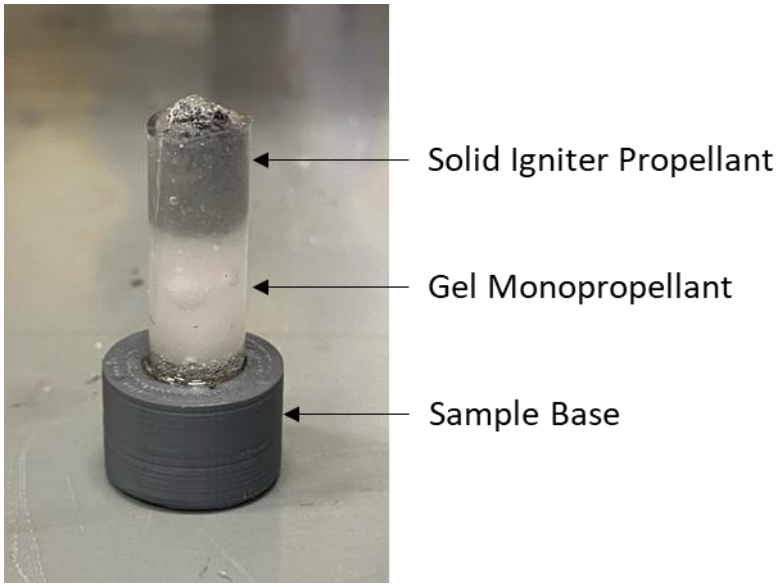

Figure 3.7: A homemade sample carrier loaded with a gel propellant and AP solid propellant igniter used for combustion studies at elevated pressure.

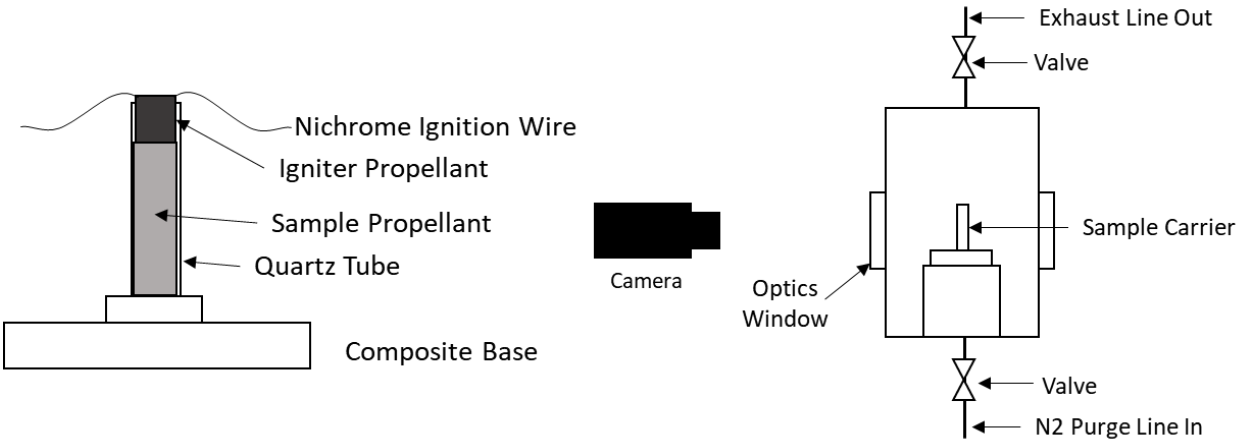

Figure 3.8: A schematic of the strand burner sample carrier (left) and the camera and apparatus configuration (right).

4. Material Characterization

This chapter describes the findings of experiments conducted to characterize the material properties of the gel monopropellants. The rheological, electrochemical, and thermal properties were investigated to understand their response in changes to oxidizer content, e.g., the incremental replacement of LP with AP at a fixed polymer to oxidizer ratio, and in turn provide context to trends seen in the combustion experiments detailed later in this thesis.

4.1. Rheological Study

Experiments conducted to observe the flow properties of the monopropellants were completed to understand the plumbing requirements in their employment and were completed in the Virginia Tech Material Characterization Facility using a TA Instruments Discover HR-30 Rheometer with a Peltier Plate and a 25mm sandblasted parallel plate fixture. Rotational oscillations at angular frequencies ranging from 0.1 to 100 $rad \cdot s^{-1}$ were applied to samples of each monopropellant, which were placed between the plates at a separation distance of 1000 μm, to collect complex viscosity data as a function of shear rate. These experiments were completed at temperatures of 20°C, 0°C, and -20°C to encompass a sample range of conditions the propellants may be subjected to in operation.

Results of the rheology study can be found in Figure 4.1. For all ECGPs, viscosity decreases with increasing angular velocity, displaying that they behave in a shear-thinning manner. Viscosity increases with decreasing temperature. At 20°C, the rate of change of complex viscosity with respect to angular velocity decreases with the addition of AP, indicating that increasing AP content results in less sensitivity to changes in applied shear forces. At -20°C, the

trend follows that increasing AP content decreases complex viscosity, as ECGP-4 possesses the highest viscosity and ECGP-8 the lowest.

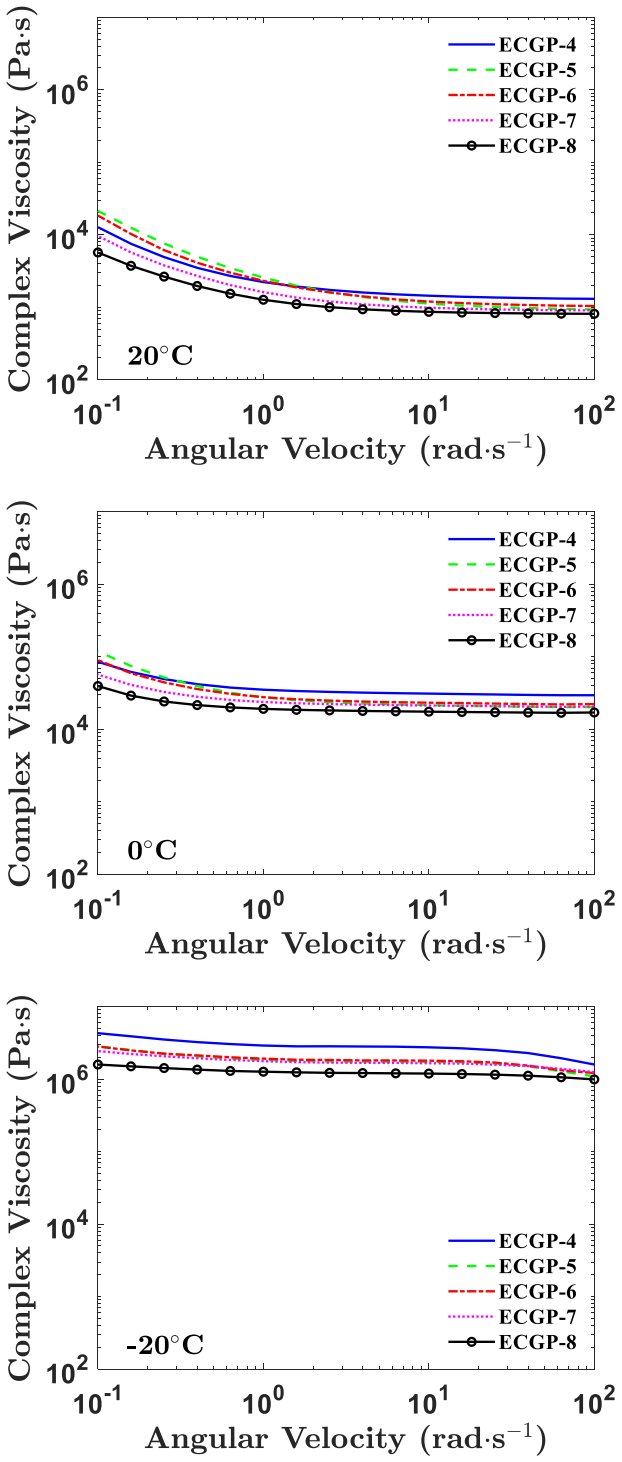

Figure 4.1: Viscosity Data for Propellants at 20˚C (top), 0˚C (middle), and -20˚C (bottom).

4.2. Electrochemical Impedance Spectroscopy

The ionic conductivity of the gel monopropellants was characterized in the Virginia Tech Material Characterization Facility using a technique known as electrochemical impedance spectroscopy (EIS) with the frequency response analyzer (FRA) module of the Autolab PGSTAT302N potentiostat. With EIS, the resistivity of an electrically or ionically conductive material can be found via the impedance response to a small alternating current (AC) signal. The resistivity relates to the material's conductivity as its reciprocal [67]. This analysis is of interest due to the GPE monopropellants' utilization of ionic conductivity in electrolysis to decompose and ignite. Thus, data collected is used to provide insight to the trends seen in the ignition delay study, as a GPE with higher resistivity would be expected to have a longer ignition delay.

In the EIS experiment, a sample of monopropellant is placed between two cylindrical graphite electrodes that have a cross-sectional diameter of 6.32 mm and is contained within a cylindrical alumina sample carrier that has an inner diameter just slightly larger than the electrodes. The electrodes are then connected to the potentionstat, which, in the FRA mode, applies a small sinusoidal oscillating voltage potential to the sample via alternating current in frequencies ranging from 100 kHz to 0.1 Hz with ten frequency sampling points per decade. The potentiostat records the applied time dependent alternating electric potential and responding current density, which are expressed below in Equations 4.1 and 4.2 in complex notation as $\psi_s(t)$ and $j_s(t)$, respectively [67].

$$\psi_s(t) = \psi_{DC} + \psi_0 e^{i2\pi ft} \quad \textbf{(4.1)}$$

$$j_s(t) = j_{DC} + j_0 e^{i[2\pi ft - \phi(f)]} \quad \textbf{(4.2)}$$

In these equations, terms denoted by the subscript *'DC'* correspond to direct current components, which are time-invariant, the terms denoted by the naught subscript are the amplitudes of the respective measurement at the imposed oscillation frequency, and $\phi(f)$ is the phase angle between the applied voltage and current density reading as a function of frequency. The total electrochemical impedance, Z, is then determined utilizing these components in the following Euler and complex formulations [68]:

$$Z = \frac{\psi_0}{j_0} * e^{i\phi(f)} = Z' + iZ'' \qquad \textbf{(4.3)}$$

The imaginary component, $-Z''$, can be plotted as a function of the real component, Z', in a complex impedance plane plot. This plot has distinctive characteristics over specific frequency ranges. Two characteristic regions of note include a semicircle which spans high frequencies followed by a linear plot over low frequencies [69]. An example for ECGP-6 is given in Fig. 4.2. In interpreting the complex impedance plane plot, the value of real impedance at which the arc intersects with the linear region is known as the internal resistance and occurs at the point of minimum imaginary impedance [68,70].

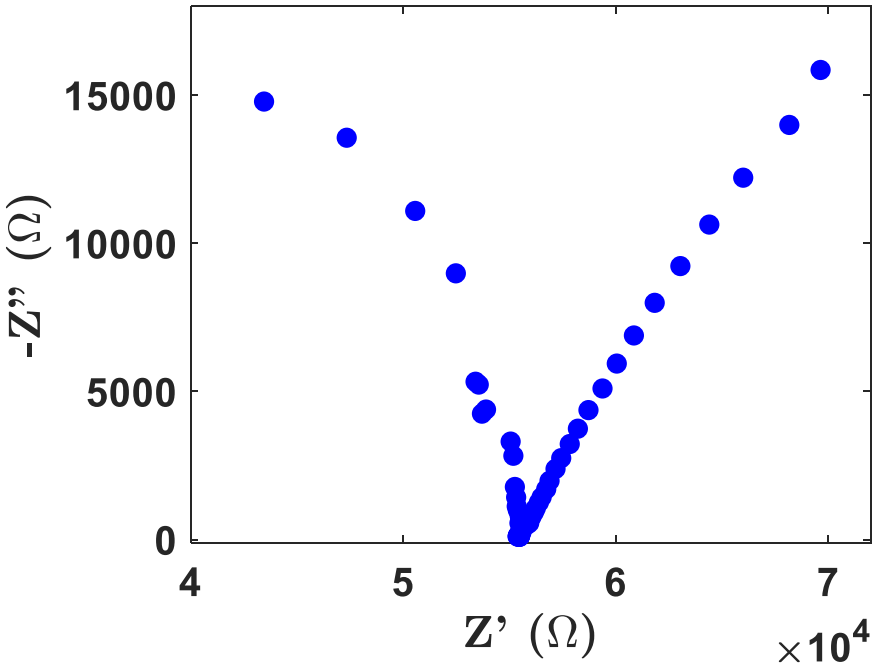

Figure 4.2: A complex impedance plane plot of ECGP-6

The internal resistance is a material property that is dependent on both the length and cross-sectional area of material subject to the applied alternating electric potential. In order to use this data to describe the electrochemical properties of the gel, it is converted to resistivity using Eqn. 3.4 below, where *R* is the measured real impedance, *A* is the area of the cross-section of the gel which is taken from the diameter of the electrodes, and *L* is taken as length of the sample between electrodes [68]. This measurement is a property that describes the ease of transportation of ions through the gels and is in units of ohmmeters.

$$\rho = \frac{RA}{L} \qquad \textbf{(4.4)}$$

The results of the EIS study include the average resistivity over three experiments for the monopropellants accompanied by the standard deviation (Appendix A). The resistivity of a material is the reciprocal of its conductivity, meaning that materials with higher resistivity more strongly resist the transportation of ions within. These findings are reported in Table 4.1. Here, it is shown that the resistivity increases with the addition of ammonium perchlorate to the gel monopropellants.

Table 4.1: Average Resistivity for ECGP Compositions.

Propellant	Average Resistivity (W*m)	Standard Deviation
ECGP-4	225.57	10.0
ECGP-5	273.19	10.9
ECGP-6	325.59	10.7
ECGP-7	389.00	5.1
ECGP-8	485.43	7.4

4.3. Simultaneous Thermogravimetric Analysis and Differential Scanning Calorimetry

The thermal characteristics of the monopropellants as well as their individual constituents were studied to understand their thermal decomposition. This was completed in a Netzsch STA 449 F5 Jupiter simultaneous thermogravimetric analysis and differential scanning calorimetry (TGA/DSC) machine. The TGA aspect of this study follows the change in mass of a material as a temperature ramp is applied in a controlled environment, describing its thermal stability. The DSC aspect records the differential rate of heat flow into or out of a substance in a controlled environment. An endotherm represents heat flow into the material, which is indicative of its melt

or evaporation, while an exotherm represents the release of heat in processes such as condensation or combustion [71]. A sample of each monopropellant and constituent was placed in an alumina crucible and into the TGA/DSC. They were subjected to a temperature ramp increasing from 20°C to 800°C at a rate of 10°C per minute with a continuous nitrogen purge. TGA/DSC results produced for the individual constituents help to provide context to the decomposition and phase changes of the gels. The results of the gels include trends in decomposition temperatures as well as phases changes and corresponding mass losses as a function of temperature.

The TGA/DSC data for the constituents of the monopropellants are found in Figure 4.3. Results for the ECGPs are subsequently depicted in Figure 4.4. Regarding the individual constituents, the initial endotherm that occurs for AP at 240°C is the transition of its orthorhombic crystalline structure to a cubic crystalline structure [72]. This is not seen to occur very prominently in the ECGPs. The primary exothermic peak of LP occurs at around 510°C and is caused by the dissociation of LP into lithium chloride (LiCl) and oxygen [73].

The initial mass loss of the propellants seen in Figure 4.4 that occurs between 80°C and 160°C is attributed to the evaporation of acetonitrile, which has a boiling point of 82°C [74]. The long cookoff of the acetonitrile is due to its retention in the gel which is a result of the strong complex it creates with ionic species and has been noted in many studies [75-77]. The primary mass loss for the monopropellants is seen to occur between about 280°C and 310°C, which corresponds to an exothermic peak in the DSC of each. The process for ECGP-4, which lacks AP, is seen to begin with the large exotherm at about 310°C that is attributed to the LP oxidizer reacting with the polymer fuel to thermally decompose. As AP is introduced and increased across the subsequent monopropellants, the primary exotherm shifted to lower temperatures which is

representative of the lower decomposition temperature of AP that appears in Figure 4.3; this shows the increased influence of the interaction of AP with the fuel which begins to dominate in the thermal decomposition process. Finally, in Figure 4.4, an endotherm that is seen just above 600°C for each monopropellant occurs as a result of lithium chloride melting. In Figure 4.3, this takes place for LP on its own at 617°C [78].

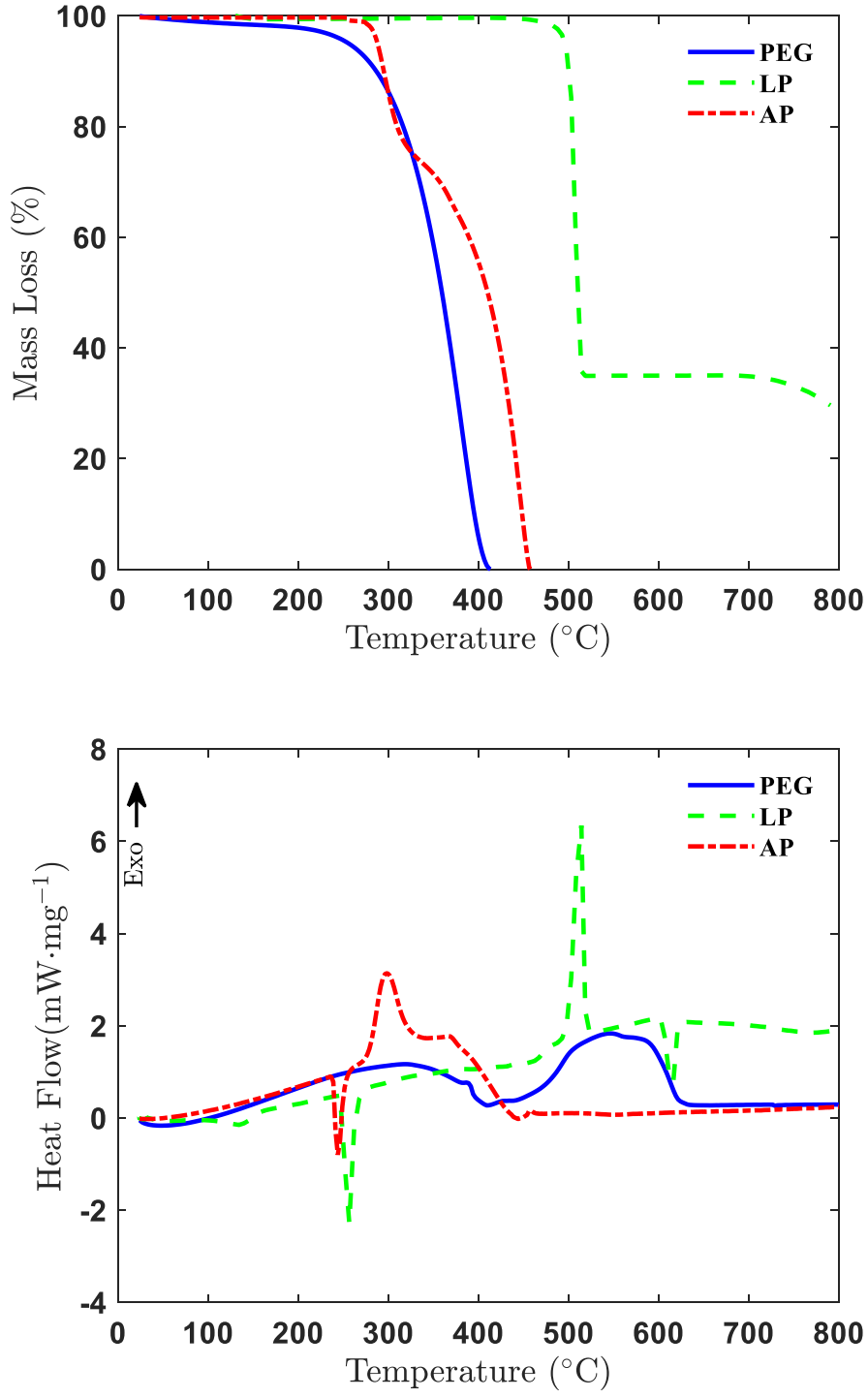

Figure 4.3: TGA (top) and DSC (bottom) results for the constituents of ECGPs.

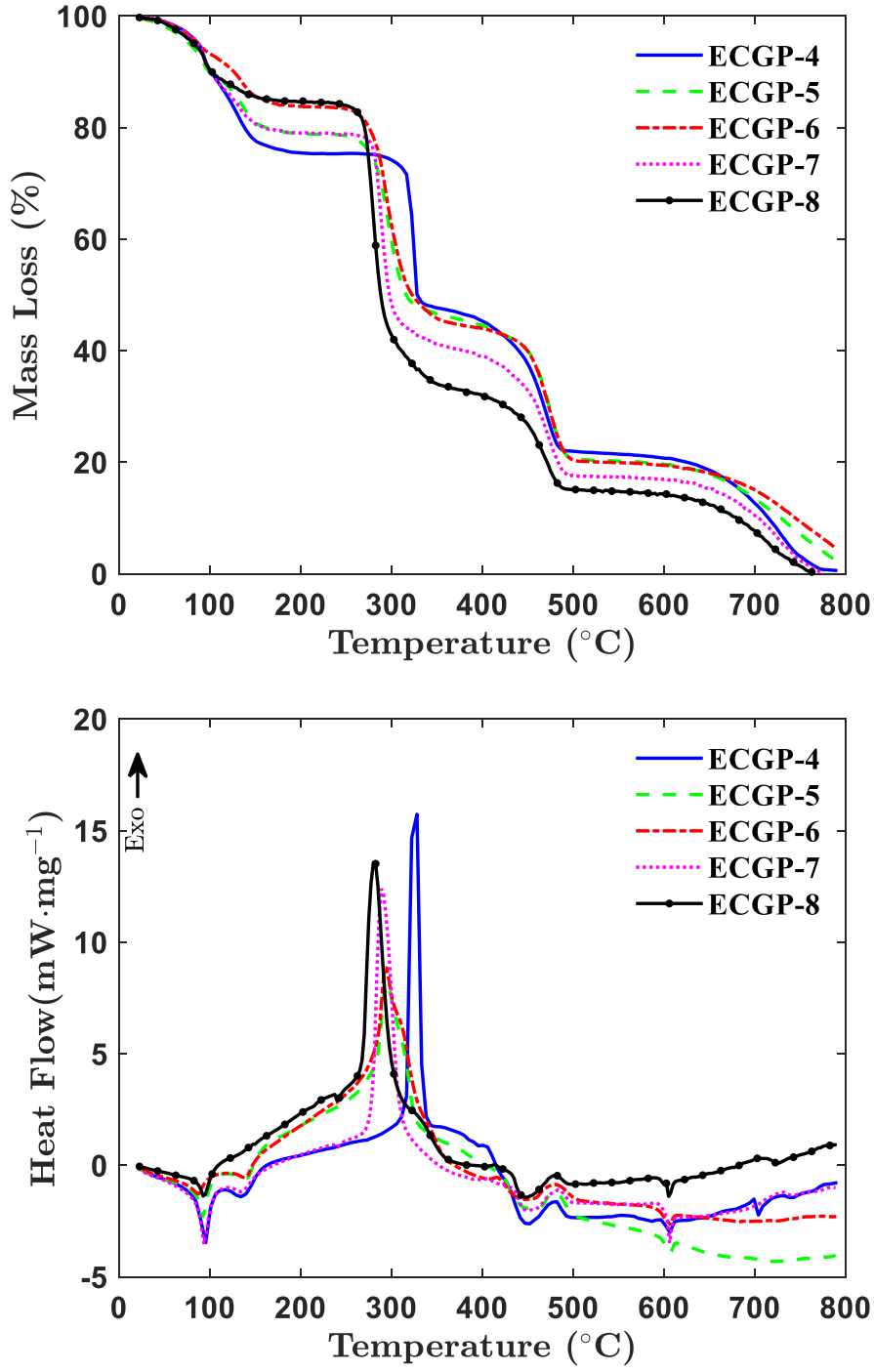

Figure 4.4: TGA (top) and DSC (bottom) results for the ECGPs.

5. Combustion Experiments

This chapter details the results and observations of the ignition delay in the electrolytic combustion of the gel monopropellants at atmospheric conditions as well as the pressurized combustion of ECGP-4, ECGP-6, and ECGP-8.

5.1. Electrolytic Ignition Delay at Atmospheric Conditions

In the electrolytic ignition study of the ECGPs, the gels were extruded along parallel electrodes which supplied voltage to the propellent. Figure 5.1 displays a sequence of images attained by high-speed cinematography of the progression of ECGP-6 through the channel of the ceramic block to decomposition and ignition with an applied voltage of 140V. The gel's initial contact with the powered electrode is denoted at time t = 0 seconds. The gel advanced through the channel, and at time t = 13.2 seconds, began to decompose at the gel front, which is the forward most region of the gel, and produced gases seen in the formation of bubbles. Shortly thereafter, the first sign of the propellant's ignition can be seen at time t = 13.9 seconds, as a small orange light appeared within this decomposition zone along the anode. The initial combustion of the gel was frequently observed to occur along the anode. By time t = 14.7 seconds, a full flame consumed the decomposition zone and began to regress through the unburned gel. The voltage was subsequently removed from the gel, quenching the flame.

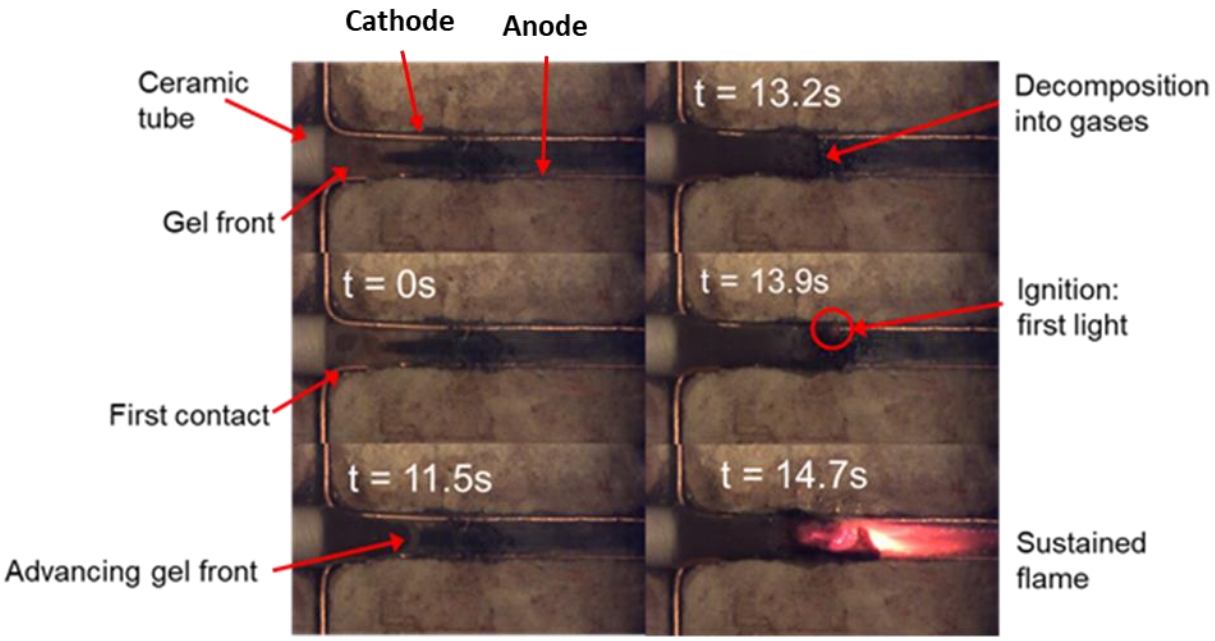

Figure 5.1: Electrolytic Combustion of ECGP-6 at 140V.

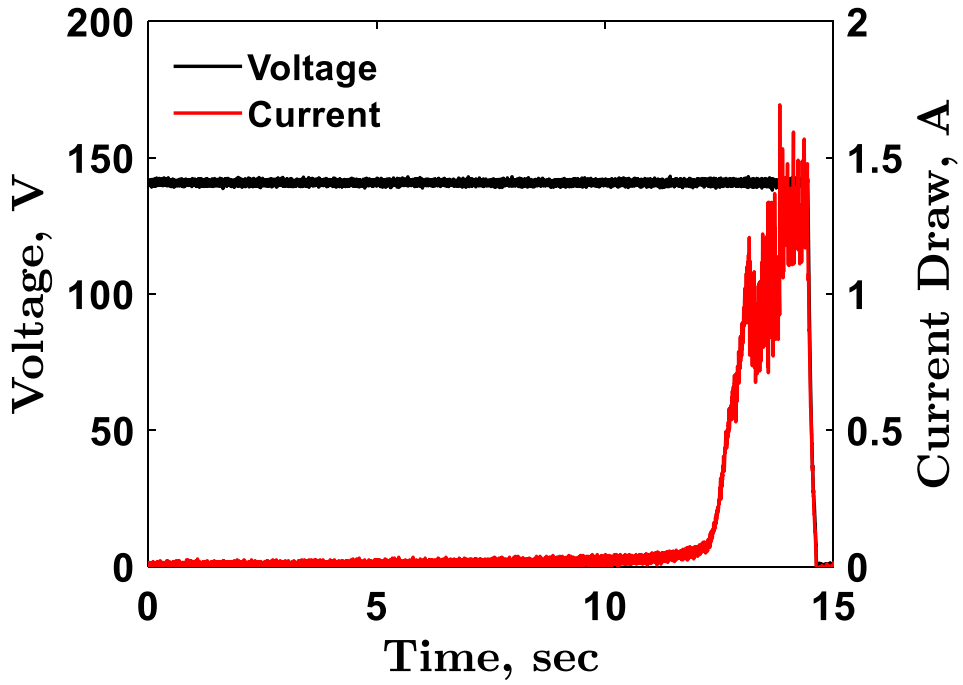

Figure 5.2: Current draw in the ignition of ECGP-6 with an applied voltage of 140V.

Results of this study can be found in Figure 5.3 which depicts the average ignition delay of each monopropellant against applied voltage at an electrode spacing of 0.635 cm, as well as ignition delay against applied voltage for ECGP-4 at two electrode spacings. For both, the error bars are representative of the standard deviation in test results, as the statistical error is greater than the observed measurement error found using the Kline-McClintock method (Appendix A).

All propellants tested displayed that increasing voltage resulted in a decrease in ignition delay times. At 120V, ECGP-4, ECGP-7, and ECGP-8 failed to ignite within two minutes, presenting only slight decomposition over this time. Data at this voltage for these gels was determined to be unreasonable to pursue, as the increasing standard deviation for their ignition delays as voltage decreased implies a high degree of unreliability. Of the propellants that contain AP, ECGP-5 and ECGP-6 are shown to experience the lowest sensitivity to changes in voltage and display the shortest ignition delay times, while ECGP-7 and ECGP-8 displayed higher sensitivities to changing voltage and longer ignition delay times. ECGP-4 is then seen to have the highest sensitivity to changing voltage as well as ignition delay times similar to that of ECGP-8. The sensitivity shown by ECGP-4 can be expected, as it is the most conductive of the monopropellants, leading to higher sensitivity to electrochemical reactions. These observations suggest that the presence of AP in small amounts enhanced the decomposition and ignition mechanisms of the propellant, however, as AP content continues to increase, the ignition delay increased across voltages.

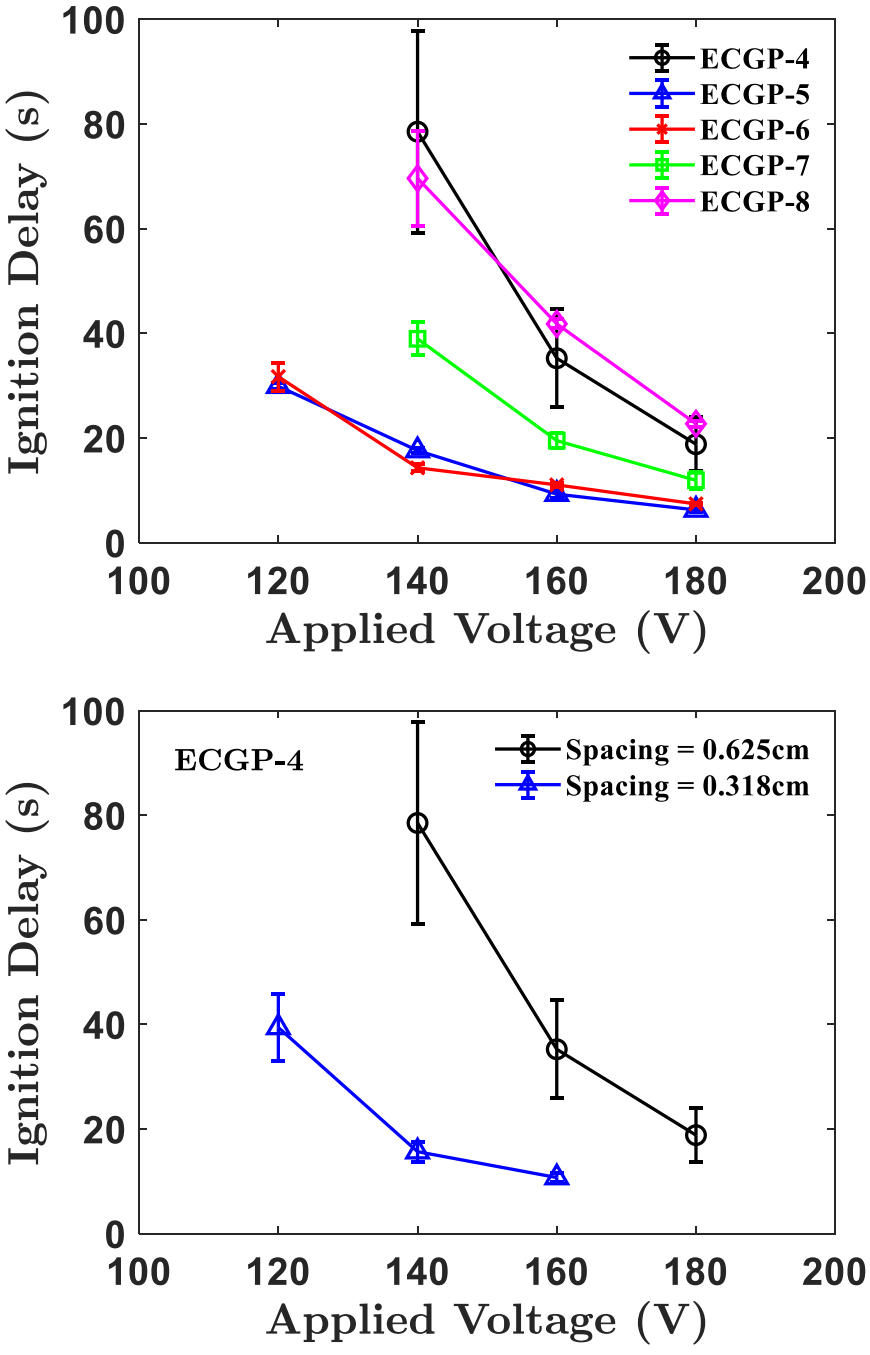

Figure 5.3: Ignition Delay data for ECGPs.

Ignition mechanisms of the monopropellants can be described as competing electrolytic and thermal processes which facilitate decomposition and combustion. The electrolytic reaction

occurs as a result of the transportation of the lithium or ammonium and perchlorate ions to the cathode and anode, respectively, where oxidation-reduction reactions occur.

As previously described, LP is broken down into its Li^+ and ClO_4^- ions when complexed with a gel polymer such as PEG to form a gel polymer electrolyte [79]. This occurs due to the donation of electrons from the oxygen-rich polymer, which provides an environment suitable for ionic separation [44,80]. This process is depicted in Equation 5.1 [79]. As stated in section 1.4, when the GPE is charged via an applied voltage, the lithium cations are transported to the cathode, where they are reduced in an exothermic oxidation-reduction reaction to gain an electron [81]. This process is described in Equation 5.2 [21,82,83].

$$LiClO_4 \rightarrow Li^+ + ClO_4^- \quad \textbf{(5.1)}$$

$$Li^+ + e^- \rightarrow Li \quad \textbf{(5.2)}$$

Ammonium perchlorate follows a similar mechanism, where the ions of NH_4^+ and ClO_4^- are produced as the GPE complex is formed [84,85]. The application of a voltage leads to the transportation of the ammonium cation to the cathode where it acquires an electron and is reduced, producing hydrogen gas [86]. These steps are depicted in Equations 5.3 and 5.4, respectively.

$$NH_4ClO_4 \rightarrow NH_4^+ + ClO_4^- \quad \textbf{(5.3)}$$

$$NH_4^+ + e^- \rightarrow \frac{1}{2}H_2 + NH_3 \quad \textbf{(5.4)}$$

The ionic conductivity is primarily driven by the transportation of the Li^+ ions, as the larger perchlorate anions have difficulty passing through the conductive medium, however, their transportation has a limited contribution as well [79,82,83]. Upon charge of the GPE, ClO_4^- ions of both oxidizer salts undergo two mechanisms in the electrochemical reaction. In the first, it is transported to the anode, where it is oxidized to produce chlorine dioxide according to the process described in Equation 5.5 [87]. The second mechanism results from excess oxidizer salt suspended in the saturated GPE, which enters its molten phase. Here, the remaining perchlorate anions electrolytically oxidize to produce chlorine and oxygen, as shown in Equation 5.6 [82].

$$\mathrm{ClO_4^-} \rightarrow ClO_2 + O_2 + e^- \quad \textbf{(5.5)}$$

$$\mathrm{ClO_4^-} \rightarrow \frac{1}{2}Cl_2 + 2O_2 + e^- \quad \textbf{(5.6)}$$

As the ions are transported to the electrodes in the presence of the applied voltage, the current drawn exponentially increases to a peak, which is believed to be concurrent with the monopropellant's ignition. This is supported by Wu and Yetter in their experiments detailing the

electrolytic ignition of a HAN solution, where a current spike coincided with the ignition of their monopropellant [36]. A representation of this phenomenon is depicted in Figure 5.2 for the same experiment of ECGP-6 shown in Figure 5.1 with an applied voltage of 140V. Here, the onset of the increase in current occurred once contact was established between the gel and electrodes; as the propellant decomposed into gases, its temperature was raised. This led to increased conductivity and allowed ions to transfer across the medium more quickly to their respective electrode, which rapidly increased the current drawn. In the example depicted in Figure 5.2, the maximum current drawn through the propellant is 1.7A.

Per the simultaneous TGA/DSC results previously discussed, the rise in temperature during electrolysis and as a result of ohmic heating allows for AP to freely react with the polymer fuel, which promotes the ignition of the propellant. The increase in resistivity with the addition of AP leads to a decrease in both ohmic heating and conductivity, which reduces the rate at which electrolysis can occur. The competition between electrolytic and thermal mechanisms is found to enhance the ignition delay of the gels through the low AP content formulations, however it begins to impact the process negatively thereafter. The electrolysis-dominated ignition is further discussed by recent work carried out at the University of California Riverside in a collaborative effort to support this research. With the use of a FLIR thermal camera, it was found that temperature changes were localized at the cathode as opposed to the presence of a temperature gradient between the electrodes. This depicts the exothermic reaction that occurs in the electrochemical reaction of the lithium ions [88].

The decrease in electrode spacing, which decreased the volume of gel subjected to the voltage potential, caused the ignition delay across voltages for ECGP-4 to decrease. This is similar to the phenomenon observed in the studies completed by Khare et. al. and Lei Li et. al., where a

decrease in propellant or droplet volume was found to decrease the ignition delay due to the increased current density [38,40]. Khare et. al. explains that increasing the current density both facilitates the electrolytic decomposition and increases ohmic heating, leading to quicker combustion of the propellant [38]. Studies have also been completed to enhance the electrolysis of water and have shown that increasing current density at fixed voltages increases the rate of production of hydrogen gas, further supporting this factor as a facilitator for electrolytic reactions [89].

5.2. Combustion at Elevated Pressures

The combustions of ECGP-4, ECGP-6, and ECGP-8 were studied under pressure in an optically accessible strand burner with a continuous nitrogen purge environment to determine their PDLs and average burn rate at the respective PDL. Determining the PDL and related burn rate of the propellant is an important safety measure to consider when designing a rocket propulsion system that utilizes solid-like propellants so as to avoid accidental burnback, which may lead to catastrophic failure. The regression rate was determined using a burn trajectory by measuring the distance that the center of the gel front advanced toward the 3D printed base of the sample carrier at multiple time intervals. Using the ImageJ image and video processing program and knowledge of a reference distance X_{ref} = 15.7 mm, a pixel length scale was determined. Figure 5.4 shows the tracked regression of ECGP-8 at a pressure of 0.345 MPa. Time t = 0 seconds serves as a reference at which the igniter propellant has been depleted and the gel is first seen burning on its own. Between times t = 15.3 and t = 45.3 seconds, the center of the gel front is seen to regress approximately 16.1 mm. Time t = 61.2 seconds shows the end of the propellant burn, at which point the gel was entirely depleted.

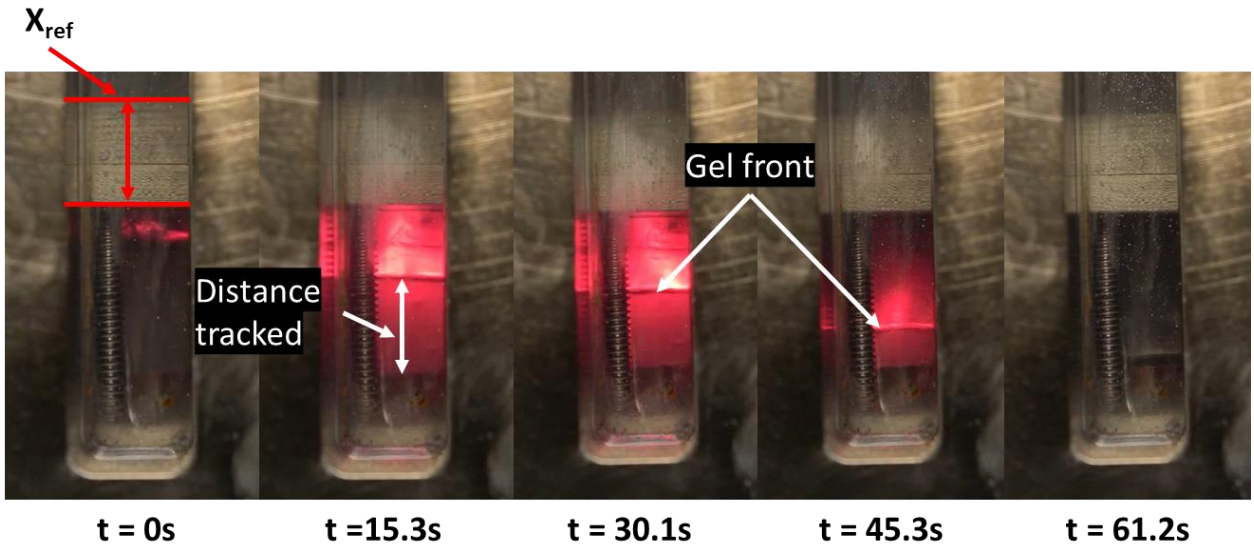

Figure 5.4: Regression of ECGP-8 at 0.345 MPa.

Table 5.1: Pressure Deflagration Limit and Regression Rate for Select Candidates.

Candidate Name	PDL (MPa)	Average Regression Rate at PDL (mm/s)	Standard Deviation
ECGP-4	2.41	0.637	0.13
ECGP-6	1.03	0.896	0.11
ECGP-8	0.345	0.357	0.0077

The combustion front of ECGP-4 was found to quench on its own for pressures below 2.41 MPa. Once ignited at 2.41 MPa, ECGP-4 regressed at a rate of about 0.637 $mm \cdot s^{-1}$. This was determined to be the PDL of the propellant. As expected, the increase in AP, whose thermal decomposition was shown to be lower than LP in the earlier TGA/DSC study, led to lower PDLs in ECGP-6 and ECGP-8. ECGP-6 quenched under its observed PDL of 1.03 MPa and regressed at this pressure at a burn rate of about 0.896 $mm \cdot s^{-1}$. Finally, the PDL of ECGP-8 was

determined to be 0.345 MPa, at which point it regressed at a rate of 0.357 mm·s^{-1}. These results are recorded in Table 5.1 alongside their respective standard deviations, and while this study does not provide a direct comparison between the burn rates of tested gels as their PDLs occur at different pressures, those with a higher AP content can be expected to have a faster regression at the same pressure. The burn rate of monopropellants, r_b, has been demonstrated to be dependent on the chamber pressure, P, by the empirical preexponential term a, and exponential factor n according to Equation 5.7 [90].

$$r_b = aP^n \quad \textbf{(5.7)}$$

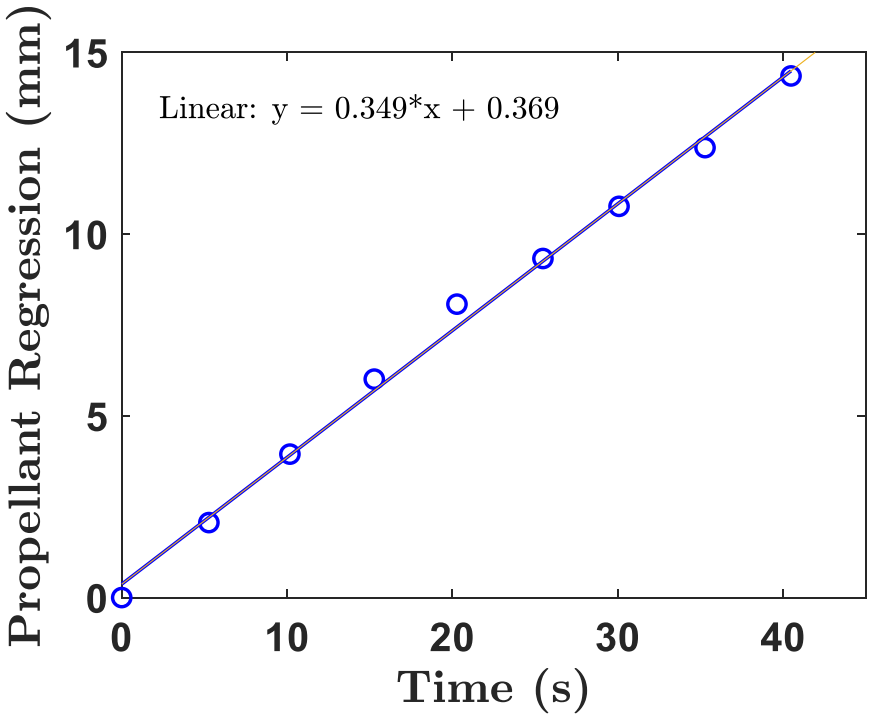

Figure 5.5: Representative Burn Trajectory of ECGP-8 at 0.345 MPa.

In the experiments, the flame of the propellant was seen to be small and present just at the surface of the gel. Occasional flares would project from the surface as the propellant regressed, which may be a result of possible bubbles exhausting as they are exposed. Figure 5.5 depicts a sample burn trajectory that was used in determining the average burn rate of ECGP-8 at its PDL, where the slope of the linear regression is the burn rate of this particular experiment.

6. Conclusions and Recommended Future Work

A family of five electrically controlled gel propellants with varying oxidizer content was developed and their material and combustion properties were assessed. The first monopropellant studied utilized only lithium perchlorate as the oxidizer salt, and subsequent candidates saw the incremental addition of AP at a fixed polymer-to-oxidizer mass ratio up to 35% AP of the total oxidizer mass. The ECGPs were demonstrated to ignite and extinguish with the application and removal of a voltage potential.

The composition of the monopropellants is derived from the concept of a gel polymer electrolyte, which is an ionically conductive material commonly used in energy storage applications that utilizes ionic salts complexed with a low molecular weight polymer. When a voltage is applied to the monopropellant, it undergoes an electrochemical reaction known as electrolysis. The ions of the oxidizer salts are transported to the electrodes where they experience an exothermic oxidation-reduction reaction, leading to the combustion of the gel.

The monopropellants were characterized materially to describe their rheological, electrochemical, and thermal properties as a function of oxidizer content to provide insight into their combustion characteristics. It was found that the monopropellants behave as thixotropic, or shear-thinning materials in the application of a shear stress, which is expected for a non-Newtonian gel. The increase in AP content was shown to decrease the conductivity of the gels, which had a direct impact on their electrolytic and thermal ignition mechanisms. In the study of their thermal stability, the increase in AP content was shown to shift the primary exothermic decomposition of the monopropellants to lower temperatures. This was a direct result of the increasing amount of AP available to decompose and interact with the polymer fuel, which occurred for a lower temperature than the exothermic decomposition of the LP oxidizer salt.

In the assessment of their combustion properties, the monopropellants were observed to undergo an electrolytic reaction with an applied voltage potential. With the presence of a competing thermal mechanism due to ohmic heating, the monopropellants decomposed and ignited. The ignition delay time, described as the time between the gel's initial contact with powered electrodes and the earliest sign of light, was characterized for each monopropellant over voltages ranging from 120V to 180V in 20V increments. Trends included the decrease in ignition delay with increasing voltage for all monopropellants studied. The presence of small amounts of AP was found to assist in the ignition of the gels, however as AP content continued to increase, the ignition process was hindered. The effect of electrode spacing was also assessed for one propellant candidate and displayed that the increase in current density as spacing decreased led to quicker ignition. Additionally, the combustion of three of the monopropellant candidates were selected to be examined under pressure to determine their pressure deflagration limits and burn rates, finding that increasing AP content decreased the PDL of the monopropellant.

Recommended work in the continuation of this research include:

- Mass spectroscopy of combustion products in both electrolytic and thermal decomposition of the monopropellants.
- Exploration of the impact of other oxidizer constituents, such as ammonium nitrate and lithium nitrate.
- Exploration of the impact of energetic additives, such as boron, aluminum, and carbon nanotubes.
- Characterize the dependence of the feed rate of the gels on its electrolytic ignition delay

- Integration of the monopropellants into a pressurized thruster that utilizes electrolytic ignition to further realize their application and potential.

Bibliography

[1] Sutton, G. P., and Biblarz, O., *Rocket Propulsion Elements*, 9th ed., John Wiley and Sons, New Jersey, 2017, Chaps. 1, 7, 13, 19.

ISBN 1118753658

[2] Hill, P. G., and Peterson, C. R., *Mechanics and Thermodynamics of Propulsion,* 2nd ed., Addison-Wesley, Massachusetts, 1992, Chaps. 1, 10, 12.

ISBN 0-201-14659-2

[3] Umholtz, P. D., "The History of Solid Rocket Propulsion and Aerojet", AFRL-PR-ED-TP-FY99-0088, Portolo Valley, CA, April 1999.

[4] Clark, J. D., *Ignition! An Informal History of Liquid Rocket Propellants,* Rutgers University Press, New Jersey, 1972.

ISBN 0-8135-0725-1

[5] Price, T. W., Evans, D. D., "The Status of Monopropellant Hydrazine Technology", NASA TR-32-1227, Pasadena, CA, February 1968.

[6] Morgan, O. M., Meinhardt, D. S., "Monopropellant Selection Criteria—Hydrazine and Other Options", *Proceedings of the 35th AIAA/ASME/SAE/ASEE Joint Propulsion Conference and Exhibit,* AIAA, Los Angeles, CA, 1999.

https://doi.org/10.2514/6.1999-2595

[7] Gohardani, A. S., Stanojev, J., Demairé, A., Anflo, K., Persson, M., Wingborg, N., Nilsson, C., "Green Space Propulsion: Opportunities and Prospects", *Progress in Aerospace Sciences,* Vol. 71, 2014, pp. 128 – 149.

https://doi.org/10.2514/6.1999-2595

[8] Larsson, A., Wingborg, N., “Green Propellants Based on Ammonium Dinitramide (ADN)”, *Advances in Spacecraft Technologies,* edited by J. Hall, InTech, Croatia, 2011, pp. 139 – 154. ISBN 978-953-307-551-8

[9] Hawkins, T. W., Brand, A. J., McKay, M. B., Tinnirello, M., “Reduced Toxicity, High Performance Monopropellant at the U.S. Air Force Research Laboratory”, AFRL-RZ-ED-TP-2010-219, Huntsville, AL, May 2010.

[10] Marshall, W. M., Deans, M. C., “Recommended Figures of Merit for Green Monopropellants”, *Proceedings of the 49th AIAA/ASME/SAE/ASEE Joint Propulsion Conference,* AIAA, San Jose, CA, 2013.
https://doi.org/10.2514/6.2013-3722

[11] Sackheim, R L., Masse, R. K., “Green Propulsion Advancement: Challenging the Maturity of Monopropellant Hydrazine”, *Journal of Propulsion and Power,* Vol. 30, No. 2, 2014, pp. 265 – 276.
https://doi.org/10.2514/1.B35086

[12] Freudenmann, D., Ciezki, H. K., “ADN and HAN-Based Monopropellants – A Minireview on Compatibility and Chemical Stability in Aqueous Media”, *Propellants, Explosives, Pyrotechnics,* Vol. 44, No. 9, 2019, pp. 1084 – 1089.
https://doi.org/10.1002/prep.201900127

[13] Meinhardt, D. S., Brewster, G., Christofferson, S., Wucherer, E. J., “Development and Testing of New, HAN-Based Monopropellants in Small Rocket Thrusters”, *Proceedings of the 34th AIAA/ASME/SAE/ASEE Joint Propulsion Conference and Exhibit,* AIAA, Cleveland, OH, 1998.
https://doi.org/10.2514/6.1998-4006

[14] Jankovsky, R. S., “HAN-Based Monopropellant Assessment for Spacecraft”, NASA TM-107287, 1996.

[15] Risha, G. A., Yetter, R. A., Yang, V., “Electrolytic-Induced Decomposition and Igntition of HAN-Based Liquid Monopropellants”, *International Journal of Energetic Materials and Chemical Propulsion,* Vol. 6, No. 5, 2007, pp. 575 – 588. https://doi.org/10.1615/IntJEnergeticMaterialsChemProp.v6.i5.30

[16] IUPAC. Compendium of Chemical Terminology, 2nd ed. (the "Gold Book"). Compiled by A. D. McNaught and A. Wilkinson. Blackwell Scientific Publications, Oxford (1997). Online version (2019-) created by S. J. Chalk. ISBN 0-9678550-9-8. https://doi.org/10.1351/goldbook.

[17] Natan, B., Rahimi, S., “The Status of Gel Propulsion in Year 2000”, *International Journal of Energetic Materials and Chemical Propulsion,* Vol. 5, No. 1-6, 2002, pp. 172-194. https://doi.org/10.1615/IntJEnergeticMaterialsChemProp.v5.i1-6.200

[18] Natan, B., Hasan, D., “Advances in Gel Propulsion”, *International Journal of Energetic Materials and Chemical Propulsion,* Vol. 18, No. 4, 2019, pp. 303–323. https://doi.org/10.1615/IntJEnergeticMaterialsChemProp.2019028375

[19] Hodge, K., Crofoot, T., Nelson, S., “Gelled Propellants for Tactical Missile Applications”, *Proceedings of the 35th Joint Propulsion Conference and Exhibit,* AIAA, Los Angeles, CA, 1999. https://doi.org/10.2514/6.1999-2976

[20] Ciezki, H. K., Naumann, K. W., Weiser, V., “Status of Gel Propulsion in the Year 2010 With a Special View on the German Activities”, *The German Aeronautical and Space Congress,* Hamburg, Germany, 2010.

[21] Kotobuki, M., “Polymer Electrolytes: State of the Art”, *Polymer Electrolytes: Characterization Techniques and Energy Applications,* edited by T. Winie, A. K. Arof, and S. Thomas, Wiley-VCH Verlag GmbH & Co., Weinheim, Germany, 2020, pp. 1-17.
ISBN 978-3-527-80543-3

[22] Petty, W. L., “Variation in Shell 405 Catalyst Physical Characteristics, Test Catalyst Preparation”, AFRPL-TR-73-56, 1973.
https://doi.org/10.21236/AD0769888

[23] Wood, S. E., Bryant, J. T., “Decomposition of Hydrazine on Shell 405 Catalyst at High Pressure”, *Industrial & Engineering Chemistry Product Research and Development,* Vol. 12, No. 2, 1973, pp. 117–122.
https://doi.org/10.1021/i360046a004

[24] Schmidt, E. W., Wucherer, E. J., “Hydrazine(s) vs. Nontoxic Propellants – Where Do We Stand Now?”, *Proceedings of the 2nd International Conference on Green Propellants for Space Propulsion (ESA SP – 557),* ESA, Cagliari, Sardinia, Italy, 2004.

[25] Amrousse, R., Hori, K., Fetimi, W., Farhat, K., “HAN and ADN as Ionic Liquid Monopropellants: Thermal and Catalytic Decomposition Processes”, *Applied Catalysis B: Environmental,* Vol. 127, October 2012, pp. 121 – 128.
https://doi.org/10.1016/j.apcatb.2014.03.050

[26] Negri, M., Wilhelm, M., Hendrich, C., Wingborg, N., Gediminas, Adelöw, L., Maleix, C., Chabernaud, P., Brahmi, R., Beauchet, R., Batonneau, Y., Kappenstein, C., Koopmans, R., Schuh, S., Bartok, T., Scharlemann, C., Gotzig, U., Schwentenwein, M., "New technologies for ammonium dinitramide based monopropellant thrusters – The project RHEFORM", *Acta Astronautica,* Vol. 143, February 2018, pp. 105 – 117. https://doi.org/10.1016/j.actaastro.2017.11.016

[27] Amrousse, R., Katsumi, T., Niboshi, Y., Azuma, N., Bachar, A., Hori, K., "Performance and Deactivation of Ir-Based Catalyst During Hydroxylammonium Nitrate Catalytic Decomposition", *Applied Catalysis A: General,* Vol. 452, February 2013, pp. 64 – 68. https://doi.org/10.1016/j.apcata.2012.11.038

[28] Courthéoux, L., Amariei, D., Rossignol, S., Kappenstein, C., "Thermal and Catalytic Decomposition of HNF and HAN Liquid Ionic as Propellants", *Applied Catalysis B: Environmental,* Vol. 62, No. 3-4, 2006, pp. 217 – 225. https://doi.org/10.1016/j.apcatb.2005.07.016

[29] Negri, M., "Replacement of Hydrazine: Overview and First Results of the H2020 Project Rheform", *Proceedings from the 6th EUROPEAN CONFERENCE FOR AERONAUTICS AND SPACE SCIENCES,* EUCASS, Kraków, Poland, 2015.

[30] Maleix, C., Chabernaud, P., Brahmi, R., Beauchet, R., Batonneau, Y., Kappenstein, C., Schwentenwein, M., Koopmans, R., Schuh, S., Scharlemann, C., "Development of Catalytic Materials for Decomposition of ADN – Based Monopropellants", *Acta Astronautica,* Vol. 158, May 2019, pp. 407 – 415. https://doi.org/10.1016/j.actaastro.2019.03.033

[31] Wilhelm, M., Negri, M., Ciezki, H., Schlechtriem, S., “Preliminary tests on thermal ignition of ADN-based liquid monopropellants”, *Acta Astronautica,* Vol. 158, May 2019, pp. 388 – 396. https://doi.org/10.1016/j.actaastro.2018.05.057

[32] Chai, W. S., Cheah, K. H., Wu, M., Koh, K. S., Sun, D., Meng, H., “A review on hydroxylammonium nitrate (HAN) decomposition techniques for propulsion application”, *Acta Astronautica,* Vol. 196, July 2022, pp. 194 – 214. https://doi.org/10.1016/j.actaastro.2022.04.011

[33] Breen, B. P., Gerstein, M., McLain, M. A., “Electrolytic Ignition System for Monopropellants”, AFRPL TR- 69-247, 1970.

[34] Vosen, S. R., “Concentration and Pressure Effects on the Decomposition Rate of Aqueous Hydroxylammonium Nitrate Solutions”, *Combustion Science and Technology,* Vol. 68, No. 4-6, 1989, pp. 85 – 99. https://doi.org/10.1080/00102208908924070

[35] Carleton, F. B., Klein, N., Krallis, K., Weinberg, F. J., “Initiating Reaction in Liquid Propellants by Focused Laser Beams”, *Combustion Science and Technology,* Vol. 88, No. 1, 1993, pp. 33 – 41. https://doi.org/10.1080/00102209308947226

[36] Wu, M., Yetter, R. A., “A novel electrolytic ignition monopropellant microthruster based on low temperature co-fired ceramic tape technology”, *Lab on a Chip,* Vol. 9, No. 7, 2009, pp. 910 – 916. https://doi.org/10.1039/B812737A

[37] Rahman, A., Chin, J., Kabir, F., Hung, Y. M., “Characterisation and thrust measurements from electrolytic decomposition of Ammonium Dinitramide (ADN) based liquid monopropellant FLP-103 in MEMS thrusters”, *Chinese Journal of Chemical Engineering,* Vol. 26, No. 9, 2018, pp. 1992 – 2002.
https://doi.org/10.1016/j.cjche.2017.09.016

[38] Khare, P., Yang, V., Meng, H., Risha, G. A., Yetter, R. A., “Thermal and Electrolytic Decomposition and Ignition of HAN-Water Solutions”, *Combustion Science and Technology,* Vol. 187, No. 7, 2015, pp. 1065 – 1078.
https://doi.org/10.1080/00102202.2014.993033

[39] Koh, K. S., Chin, J., Wahida Ku Chik, T. F., “Role of electrodes in ambient electrolytic decomposition of hydroxylammonium nitrate (HAN) solutions”, *Propulsion and Power Research,* Vol. 2, No. 3, 2013, pp. 194 – 200.
https://doi.org/10.1016/j.jppr.2013.07.002

[40] Li, L., Li, G., Li, H., Yao, Z., “Effect of voltage and droplet size on electrical ignition characteristics of ADN-based liquid propellant droplet”, *Aerospace Science and Technology,* Vol. 93, October 2019.
https://doi.org/10.1016/j.ast.2019.105314

[41] Li, H., Li, G., Li, L., Wu, J., Yao, Z, Zhang, T., “Combustion characteristics and concentration measurement of ADN-based liquid propellant with electrical ignition method in a combustion chamber”, *Fuel,* Vol., 344, July 2023.
https://doi.org/10.1016/j.fuel.2023.128142

[42] Stephan, A. M., “Review on gel polymer electrolytes for lithium batteries”, *European Polymer Journal,* Vol. 42, No. 1, 2006, pp. 21 – 42.

https://doi.org/10.1016/j.eurpolymj.2005.09.017

[43] Xue, Z., He, D., Xie, X., “Poly(ethylene oxide)-based electrolytes for lithium-ion batteries”, *Journal of Materials Chemistry A,* Vol. 3, No. 38, 2015, pp. 19218 – 19253.

https://doi.org/10.1039/C5TA03471J

[44] Mao, G., Saboungi, M.-L., Price, D. L., Badyal, Y. S., Fischer, H. E., “Lithium environment in PEO-$LiClO_4$ polymer electrolyte”, *Europhysics Letters,* Vol. 54, No. 3, 2001, pp. 347 – 353.

https://doi.org/10.1209/epl/i2001-00249-7

[45] Li, W., Pang, Y., Liu, J., Liu, G., Wang, Y., Xia, Y., “A PEO-based gel polymer electrolyte for lithium ion batteries”, *RSC Advances,* Vol. 7, No. 38, 2017, pp. 23494 – 23501.

https://doi.org/10.1039/C7RA02603J

[46] Sudhakar, Y. N., Selvakumar, M., “Lithium perchlorate doped plasticized chitosan and starch blend as biodegradable polymer electrolyte for supercapacitors”, *Electrochimica Acta,* Vol. 78, September 2012, pp. 398 – 405.

https://doi.org/10.1016/j.electacta.2012.06.032

[47] Cheng, X., Pan, J., Zhao, Y., Liao, M., Peng, H., “Gel Polymer Electrolytes for Electrochemical Energy Storage”, *Advanced Energy Materials,* Vol. 8, No. 7, 2018, pp. 1702184.

https://doi.org/10.1002/aenm.201702184

[48] Jyoti, B. V. S., Naseem, M. S., Baek, S. W., Lee, H. J., Cho, S. J., “Hypergolicity and ignition delay study of gelled ethanolamine fuel”, *Combustion and Flame,* Vol. 183, September 2017, pp. 102 – 112.

https://doi.org/10.1016/j.combustflame.2017.05.007

[49] Nachmoni, G., Natan, B., “Combustion Characteristics of Gel Fuels”, *Combustion Science and Technology,* Vol. 156, No. 1, 2000, pp. 139 – 157.
https://doi.org/10.1080/00102200008947300
[50] Arnold, R., Anderson, W., “Droplet Burning of JP-8/Silica Gels”, *Proceedings from the 48th AIAA Aerospace Sciences Meeting Including the New Horizons Forum and Aerospace Exposition,* AIAA, Orlando, FL.
https://doi.org/10.2514/6.2010-421
[51] Cao, Q., Liao, W., Wu, W., Feng, F., “Combustion characteristics of inorganic kerosene gel droplet with fumed silica as gellant”, *Experimental Thermal and Fluid Science,* Vol. 103, May 2019, pp. 377 – 384.
https://doi.org/10.1016/j.expthermflusci.2019.01.031
[52] Fu, Q., Duan, R., Cui, K., Yang, L., “Spray of gelled propellants from an impinging-jet injector under different temperatures”, *Aerospace Science and Technology,* Vol. 39, December 2014, pp. 552 – 558.
https://doi.org/10.1016/j.ast.2014.07.001
[53] Guan, H., Li, G., Zhang, N., “Experimental investigation of atomization characteristics of swirling spray by ADN gelled propellant”, *Acta Astronautica,* Vol. 144, March 2018, pp. 119 – 125.
https://doi.org/10.1016/j.actaastro.2017.12.015
[54] Ma, X., Jin, S., Xie, W., Liu, Y., Zhang, W., Chen, Y., “A novel green electrically controlled solid propellant with good electrical response and high energy performance”, *Colloids and Surfaces A:Physiochemical and Engineering Aspects,* Vol. 641, May 2022, pp. 128550.
https://doi.org/10.1016/j.colsurfa.2022.128550

[55] He, Z., Xia, Z., Hu, J., Li, Y., “Lithium-Perchlorate/Polyvinyl-Alcohol-Based Aluminized Solid Propellants with Adjustable Burning Rate”, *Journal of Propulsion and Power,* Vol. 35, No. 3, 2019, pp. 512 – 519.
https://doi.org/10.2514/1.B37279

[56] Gobin, B., Harvey, N., Arnold, C., Whalen, S., Young, G., “Utilization of Ionically Conducting Polymers in Electrically Controlled Gel Monopropellants”, Journal of Propulsion and Power, Vol. 38, No. 6, 2022.
https://doi.org/10.2514/1.B38748

[57] Khoruzhii, I. V., Klyakin, G. F., Taranushich, V. A., Lachin, V. I., “A study of the electrothermal method for control over combustion velocity under atmospheric pressure of energetic condensed systems based on ammonium nitrate”, *Russian Journal of Applied Chemistry,* Vol. 80, No. 8, 2007, pp. 1295 – 1299.
https://doi.org/10.1134/S107042720708006X

[58] Gobin, B., Whalen, S., Plunkett, E. M., Godshall, G. F., Moore, R. B., Young, G., “Effect of Electrical Stimuli on Combustion Behavior of Solid Oxidizers”, *International Journal of Energetic Materials and Chemical Propulsion,* Vol. 20, No. 3, 2021, pp. 27 – 44.
https://doi.org/10.1615/IntJEnergeticMaterialsChemProp.2021038286

[59] Gnanaprakash, K., Lim, D., Yoh, J. J., “Combustion characteristics of lithium perchlorate-based electrically controlled solid propellants at elevated pressures”, *Thermochimica Acta,* Vol. 720, February 2023, pp. 179421.
https://doi.org/10.1016/j.tca.2022.179421

[60] Baird, J. K., Frederick, R. A., Jr., “Thermochemistry of Combustion in Polyvinyl Alcohol + Hydroxylammonium Nitrate”, *Aerospace,* Vol. 8, No. 5, 2021.

https://doi.org/10.3390/aerospace8050142

[61] Baird, J. K., Lang, J. R., Hiatt, A. T., Frederick, R. A., Jr., "Electrolytic Combustion in the Polyvinyl Alcohol Plus Hydroxylammonium Nitrate Solid Propellant", *Journal of Propulsion and Power,* Vol. 33, No. 6, 2017, pp. 1589 – 1590.

https://doi.org/10.2514/1.B36450

[62] Foran, G., Mankovsky, D., Verdier, N., Lepage, D., Prébé, A., Aymé-Perrot, D., Dollé, M., "The Impact of Absorbed Solvent on the Performance of Solid Polymer Electrolytes for Use in Solid-State Lithium Batteries", *iScience,* Vol. 23, No. 10, 2020.

https://doi.org/10.1016/j.isci.2020.101597

[63] Weston, J. E., Steele, B. C. H., "Effects of preparation method on properties of lithium salt-poly(ethylene oxide) polymer electrolytes", *Solid State Ionics,* Vol. 7, No. 1, 1982, pp. 81 – 88.

https://doi.org/10.1016/0167-2738(82)90073-X

[64] Gordon, S., McBride, B. J., "Computer program for calculation of complex chemical equilibrium compositions and applications", NASA RP-1311, Cleveland, OH, 1994.

[65] Zanotti, C., Giuliani, P., "Pressure deflagration limit of solid rocket propellants: Experimental results", *Combustion and Flame,* Vol. 98, No. 1-2, 1994, pp. 35 – 45.

https://doi.org/10.1016/0010-2180(94)90196-1

[66] Meier, J. H., "Novel Gel-Infused Additively Manufactured Hybrid Rocket Solid Fuels", Virginia Polytechnic Institute and State University, Blacksburg, VA, 2023.

[67] Careem, M. A., Noor, I. S. M., Arof, A. K., "Impedance Spectroscopy in Polymer Electrolyte Characterization", *Characterization Techniques and Energy Applications,* edited by T. Winie, A. K. Arof, and S. Thomas, Wiley-VCH Verlag GmbH & Co., Weinheim, Germany, 2020, pp. 23 – 64.

ISBN 978-3-527-80545-7

[68] Mei, B., Munteshari, O., Lau, J., Dunn, B., Pilon, L., "Physical Interpretations of Nyquist Plots for EDLC Electrodes and Devices", *The Journal of Physical Chemistry C,* Vol. 122, No. 1, 2018, pp. 194 – 206.
https://doi.org/10.1021/acs.jpcc.7b10582

[69] Yang, I., Kim, S., Kwon, S. H., Kim, M., Jung, J. C., "Relationships between pore size and charge transfer resistance of carbon aerogels for organic electric double-layer capacitor electrodes", *Electrochimica Acta,* Vol. 223, January 2017, pp. 21 – 30.
https://doi.org/10.1016/j.electacta.2016.11.177

[70] Lei, C., Markoulidiz, F., Ashitaka, Z., Lekakou, C., "Reduction of porous carbon/Al contact resistance for an electric double-layer capacitor (EDLC)", *Electrochimica Acta,* Vol. 92, March 2013, pp. 183 – 187.
https://doi.org/10.1016/j.electacta.2012.12.092

[71] Menczel, J. D., Judovits, L., Prime, R. B., Bair, H. E., Reading, M., Swier, S., "Differential Scanning Calorimetry (DSC)", *Thermal Analysis of Polymers,* edited by J. D. Menczel and R. B. Prime, John Wiley & Sons, New Jersey, 2009.
ISBN 978-0-471-76917-0

[72] Kubota, N., "Propellants and Explosives", 3rd ed., John Wiley and Sons, Wiley-VCH Verlag GmbH & Co., Weinheim, Germany, 2015, Chap. 4, pp. 77.
ISBN 978-3-527-69351-1

[73] Markowitz, M. M., Boryta, D. A., "The Decomposition Kinetics of Lithium Perchlorate", *The Journal of Physical Chemistry,* Vol. 65, No. 8, 1961, pp. 1419 – 1424.
https://doi.org/10.1021/j100826a034

[74] O'Donnell, J. F., Ayres, J. T., Mann, C. K., "Preparation of High Purity Acetonitrile", *Analytical Chemistry,* Vol. 37, No. 9, 1965, pp. 1161 – 1162.
https://doi.org/10.1021/ac60228a027

[75] Commarieu, B., Paolella, A., Collin-Martin, S., Gagnon, C., Vijh, A., Guerfi, A., Zaghib, K., "Solid-to-liquid transition of polycarbonate solid electrolytes in Li-metal batteries", *Journal of Power Sources,* Vol. 436, October 2019.
https://doi.org/10.1016/j.jpowsour.2019.226852

[76] Denney, J., Huang, H., "Thermal Decomposition Characteristics of PEO/LiBF4/LAGP Composite Electrolytes", *Journal of Composites Science,* Vol. 6, No. 4, 2022.
https://doi.org/10.3390/jcs6040117

[77] Yamada, Y., Furukawa, K., Sodeyama, K., Kikuchi, K., Yaegashi, M., Tateyama, Y., Yamada, A., "Unusual Stability of Acetonitrile-Based Superconcentrated Electrolytes for Fast-Charging Lithium-Ion Batteries", *Journal of the American Chemical Society,* Vol. 136, No. 13, 2014, pp. 5039 – 5046.
https://doi.org/10.1021/ja412807w

[78] Markowitz, M. M., Boryta, D. A., Stewart, H., "Lithium Perchlorate Oxygen Candle. Pyrochemical Source of Pure Oxygen", *Industrial & Engineering Chemistry Product Research and Development,* Vol. 3, No. 4, 1964, pp. 321 – 330.
https://doi.org/10.1021/i360012a016

[79] Watanabe, M., Nagano, S., Sanui, K., Ogata, N., "Ionic Conductivity of Network Polymers from Poly(ethylene oxide) Containing Lithium Perchlorate", *Polymer Journal,* Vol. 18, No. 11, 1986, pp. 809 – 817.
https://doi.org/10.1295/polymj.18.809

[80] Zhang, Z., Gong, W., Bai, Z., Wang, D., Xu, Y., Li, Z., Guo, J., Turng, L., "Oxygen-Rich Polymers as Highly Effective Positive Tribomaterials for Mechanical Energy Harvesting", *ACS Nano,* Vol. 13, No. 11, 2019, pp. 12787 – 12797.
https://doi.org/10.1021/acsnano.9b04911

[81] Rinkel, B. L. D., Hall, D. S., Temprano, I., Grey, C. P., "Electrolyte Oxidation Pathways in Lithium-Ion Batteries", *Journal of the American Chemical Society,* Vol. 142, No. 35, 2020, pp. 15058 – 15074.
https://doi.org/10.1021/jacs.0c06363

[82] Anders, U., Plambeck, J. A., "Electrochemistry of Fused Lithium Perchlorate", *Journal of the Electrochemical Society,* Vol. 115, No. 6, 1968, pp. 598 – 600.
https://doi.org/10.1149/1.2411355

[83] Watanabe, M., Togo, M., Sanui, K., Ogata, N., Kobayashi, T., Ohtaki, Z., "Ionic Conductivity of Polymer Complexes Formed by Poly(β-propiolactone) and Lithium Perchlorate", *Macromolecules,* Vol. 17, No. 12, 1984, pp. 2908 – 2912.
https://doi.org/10.1021/ma00142a079

[84] Gray, F. M., *Polymer Electrolytes,* Cambridge: Royal Society of Chemistry, Great Britain, 1997, pp. 1 – 26.
ISBN 0-85404-557-0

[85] Gray, F. M., *Solid Polymer Electrolytes: Fundamentals and Technological Applications,* Wiley VCH, New York, 1991, pp. 45 – 53.
ISBN 0-89573-772-8

[86] Berkh, O., Shacham-Diamand, Y., Gileadi, E., "Reduction of Ammonium Ion on Pt Electrodes", *Journal of The Electrochemical Society,* Vol. 155, No. 10, 2008, pp. F223 – F229

https://doi.org/10.1149/1.2967332

[87] Glass, G. E., West, R., “Formation of chlorine dioxide by the electrolytic oxidation of perchlorate anion”, *Inorganic Chemistry,* Vol. 11, No. 11, 1972, pp. 2847 – 2849.

https://doi.org/10.1021/ic50117a056

[88] Autry, H. R., Young, G., “The Effects of Oxidizer Content on Electrically Controlled Gel Polymer Electrolyte Monopropellants”, Submitted to be published in AIAA Journal of Propulsion and Power, 2023.

[89] Wang, M., Wang, Z., Guo, Z., “Water electrolysis enhanced by super gravity field for hydrogen production”, *International Journal of Hydrogen Energy,* Vol. 35, No. 8, 2010, pp. 3198 – 3205.

https://doi.org/10.1016/j.ijhydene.2010.01.128

[90] Chang, Y., Kuo, K., “Assessment of combustion characteristics and mechanism of a HAN-based liquid monopropellant”, *Proceedings of the 37th Joint Propulsion Conference and Exhibit,* AIAA, Salt Lake City, Utah, 2001.

https://doi.org/10.2514/6.2001-3272

[91] Kline, S. J., McClintock, F. A., “Describing Uncertainties in Single-Sample Experiments”, *Mechanical Engineering,* January 1953, pp. 3 – 8.

[92] Kline, S. J., “The Purpose of Uncertainty Analysis”, *The Journal of Fluids Engineering,* Vol. 107, June 1985, pp. 153 – 160.

https://doi.org/10.1115/1.3242449

Appendix A: Uncertainty Analysis

The Kline and McClintock method for uncertainty analysis was used to describe the uncertainty of measurements made throughout experimentation [91,92]. This method follows that, for a given function, *R*, of *n* variables, the uncertainty in the results is derived from the propagation of variation in its variables, as is shown in Equations A1 and A2, the latter of which is known as the second-power equation and is derived from the definition of standard deviation in a normally distributed function [91].

$$R = R(u_1, u_2, \dots, u_n) \quad \textbf{(A1)}$$

$$\delta R = \left[\left(\frac{\partial R}{\partial u_1}\delta u_1\right)^2 + \left(\frac{\partial R}{\partial u_2}\delta u_2\right)^2 + \cdots + \left(\frac{\partial R}{\partial u_n}\delta u_n\right)^2\right]^{\frac{1}{2}} \quad \textbf{(A2)}$$

The example displayed in Equations A3 and A4 depict the measurement uncertainty in the determination of the ignition delay, τ_{ign}, of the monopropellants. Here, Δn is the difference in frame number between the frame at which contact between the gel and electrodes is first established and the frame at which a flame is first depicted, and f_s is the sampling rate of the high-speed camera used in experimentation and is taken to be 250 frames per second or 0.004 s^{-1}. The frame rate is the smallest unit of measurement used and is therefore considered the uncertainty in sampling rate.

$$\tau_{ign} = \frac{\Delta n}{f_s} \qquad \textbf{(A3)}$$

$$\delta\tau_{ign} = \left[\left(\frac{\partial \tau_{ign}}{\partial f_s}\delta f_s\right)^2\right]^{\frac{1}{2}} = \left[\left(\frac{\Delta n}{f_s^2}\, f_s\right)^2\right]^{\frac{1}{2}} = \left[\left(\frac{\Delta n}{250^2}\, 250\right)^2\right]^{\frac{1}{2}} = \pm .004 \qquad \textbf{(A4)}$$

In this analysis, it was determined that the statistical error is much higher than calculated measurement uncertainties, thus, the statistical error is used to represent the uncertainty in given results.